AGU PUBLICATIONS

Journal of Advances in Modeling Earth Systems

RESEARCH ARTICLE

10.1002/2015MS000576

Climate, soil organic layer, and nitrogen jointly drive forest development after fire in the North American boreal zone

A. T. Trugman[1], N. J. Fenton[2,3], Y. Bergeron[2,3], X. Xu[4], L. R. Welp[5], and D. Medvigy[1,4]

[1]Program in Atmospheric and Oceanic Sciences, Princeton University, Princeton, New Jersey, USA, [2]Forest Research Institute, NSERC-UQAT-UQAM Industrial Chair in Sustainable Forest Management, Université du Québec en Abitibi-Témiscamingue, Rouyn-Noranda, Québec, Canada, [3]Centre d' Études sur la Forêt, Université du Québec a Montréal, Montréal, Québec, Canada, [4]Department of Geosciences, Princeton University, Princeton, New Jersey, USA, [5]Department of Earth, Atmospheric, and Planetary Sciences, Purdue University, West Lafayette, Indiana, USA

Key Points:
- We developed and validated a North American boreal forest model with a dynamic feedback between the soil organic layer and tree growth
- The soil organic layer feedback affects boreal forest broadleaf presence which impacts aboveground and soil carbon accumulation
- Higher temperatures and a thinner soil organic layer can drive increased broadleaf presence, reducing boreal forest carbon accumulation

Supporting Information:
- Data Set S1

Correspondence to:
A. T. Trugman,
att@princeton.edu

Citation:
Trugman, A. T., N. J. Fenton, Y. Bergeron, X. Xu, L. R. Welp, and D. Medvigy (2016), Climate, soil organic layer, and nitrogen jointly drive forest development after fire in the North American boreal zone, *J. Adv. Model. Earth Syst.*, *8*, 1180–1209, doi:10.1002/2015MS000576.

Received 28 OCT 2015
Accepted 29 JUN 2016
Accepted article online 1 JUL 2016
Published online 11 AUG 2016

Abstract Previous empirical work has shown that feedbacks between fire severity, soil organic layer thickness, tree recruitment, and forest growth are important factors controlling carbon accumulation after fire disturbance. However, current boreal forest models inadequately simulate this feedback. We address this deficiency by updating the ED2 model to include a dynamic feedback between soil organic layer thickness, tree recruitment, and forest growth. The model is validated against observations spanning monthly to centennial time scales and ranging from Alaska to Quebec. We then quantify differences in forest development after fire disturbance resulting from changes in soil organic layer accumulation, temperature, nitrogen availability, and atmospheric CO_2. First, we find that ED2 accurately reproduces observations when a dynamic soil organic layer is included. Second, simulations indicate that the presence of a thick soil organic layer after a mild fire disturbance decreases decomposition and productivity. The combination of the biological and physical effects increases or decreases total ecosystem carbon depending on local conditions. Third, with a 4°C temperature increase, some forests transition from undergoing succession to needleleaf forests to recruiting multiple cohorts of broadleaf trees, decreasing total ecosystem carbon by ~40% after 300 years. However, the presence of a thick soil organic layer due to a persistently mild fire regime can prevent this transition and mediate carbon losses even under warmer temperatures. Fourth, nitrogen availability regulates successional dynamics; broadleaf species are less competitive with needleleaf trees under low nitrogen regimes. Fifth, the boreal forest shows additional short-term capacity for carbon sequestration as atmospheric CO_2 increases.

1. Introduction

The boreal forest has experienced significant changes in climate over the past century. Atmospheric carbon dioxide concentrations have increased by 100 ppm since 1900 and could increase to 1000 ppm by 2100 in high-emissions scenarios [*IPCC*, 2013]. Air temperature has risen 2°C at high latitudes since 1901, and is projected to rise by an additional 2°–11°C by 2100 [*IPCC*, 2013]. In recent decades, fire frequency and severity have also increased in the western part of the North American (NA) boreal forest [*Kasischke and Turetsky*, 2006]. Over the next century, it is projected that warming temperatures and hotter drought conditions will extend the fire season length, resulting in further increases in fire frequency and larger, more severe fires in Alaska and in many parts of Canada [*Girardin et al.*, 2013; *Hinzman et al.*, 2013; *Kasischke and Turetsky*, 2006]. Projected changes in temperature and fire also have the potential to increase plant available nitrogen in the boreal forest by increasing the rate of nitrogen cycling and by changing atmospheric nitrogen deposition rates [*Weber and Flannigan*, 1997].

Models are useful tools for understanding how the complex changes in atmospheric CO_2, temperature, fire regime, and nitrogen cycling can affect NA boreal forest dynamics. However, current models often do not adequately represent complex soil processes that determine forest composition and carbon storage. Here we highlight how uncertainty surrounding interactions between the soil organic layer and aboveground forest growth can strongly affect projections of NA boreal forest carbon dynamics.

In the NA boreal forest, there is a biological feedback between fire severity, soil organic layer thickness, tree seedling survivorship, and aboveground forest growth [*Drobyshev et al.*, 2010; *Greene et al.*, 2007; *Johnstone*

and Chapin, 2006a; *Johnstone et al*., 2010; *Lafleur et al*., 2010, 2015a; *Lecomte and Bergeron*, 2005]. The residual soil organic layer depth left behind after a fire is important in secondary succession because recruits and suckers of both deciduous broadleaf species, such as trembling aspen (*Populus tremuloides* Michx.), and evergreen needleleaf species, such as black spruce (*Picea mariana* Mill.), grow more readily in the presence of exposed mineral soil [*Greene et al*., 2007; *Johnstone and Chapin*, 2006a; *Johnstone et al*., 2010; *Lafleur et al*., 2015a]. However, larger-seeded evergreen needleleaf species, such as black spruce, are able to grow on thick organic beds, albeit with higher seedling mortality rates [*Greene et al*., 2007]. As a result, frequent, severe fires that burn away most of the surface organic layer and expose the mineral soil increase deciduous broadleaf forest growth [*Johnstone and Chapin*, 2006b]. In contrast, black spruce is generally the dominant canopy tree in old forests or during secondary succession when a thick organic soil layer remains present after a fire [*Johnstone and Chapin*, 2006a; *Lecomte and Bergeron*, 2005].

While soil organic layer depth affects aboveground biomass accumulation, forest growth also controls organic layer accumulation. In broadleaf aspen forests, easily decomposable litter, lack of moss growth, and warm ground conditions increase decay rates and prevent significant accumulation of surface soil carbon [*Laganière et al*., 2010; *Légaré et al*., 2005]. However, due to a relatively deep rooting system (up to 100 cm), aspen forests tend to preserve some carbon in deeper layers within the mineral soil [*Laganière et al*., 2013]. In contrast, black spruce growth promotes continual soil organic layer accumulation through inputs of slowly decomposing, nitrogen-poor needles, understory moss growth, and cold ground conditions [*La Roi and Stringer*, 1976; *Laganière et al*., 2011]. Thus, there tends to be less soil carbon associated with aspen broadleaf forests than old black spruce forests [*Légaré et al*., 2005].

These interacting processes have only partially been incorporated into models. Models of forests in Alaska and central Canada have incorporated dynamic organic layer accumulation [*Bona et al*., 2016; *Carrasco et al*., 2006; *Yi et al*., 2010; *Zhuang et al*., 2002], NA boreal-specific tree types, and dynamic vegetation [*Euskirchen et al*., 2014; *Euskirchen et al*., 2009]. Other models have been used to study the interplay between fires [*Yue et al*., 2013], soil organic layer depth, and aboveground forest growth within subregions of Canada and Alaska [*de Groot et al*., 2003; *Terrier et al*., 2014]. Yet no NA boreal forest models applied to a range of climate gradients have coupled dynamic vegetation processes and dynamic soil organic layer accumulation, or included the effect of organic layer depth on tree seedling and sucker survivorship. How these omissions impact simulations of NA boreal carbon storage is unclear.

Ideally, models should not only account for these impacts, but also demonstrate scalability, or predictive power across space and time. There are numerous regionally varying factors that influence the response of NA boreal forests to climate change. Permafrost distribution, soil type, nitrogen availability, temperature, precipitation, and fire frequency all differ regionally throughout the NA boreal forest [*Kasischke and Turetsky*, 2006; *Reay et al*., 2008] and all exert control on aboveground forest structure [*Drobyshev et al*., 2013; *Girardin et al*., 2014], and soil carbon accumulation [*Lavoie et al*., 2005]. A scalable model accurately captures observed spatial variations in growth dynamics due to variations in environmental and climate factors over both short and long timescales.

This study has two overall objectives. First, we seek to develop a data-constrained model framework for understanding NA boreal forest development after fire disturbance. Specifically, we update the Ecosystem Demography model version 2 (ED2) to include new parameterizations for broadleaf aspen and needleleaf black spruce species-types, a dynamic soil organic layer, species-specific seedling survivorship dependent on the organic layer thickness, and species-specific litter decay rates. The model is tested against observations from throughout the NA boreal forest including eddy covariance measurements and forest inventory data in Alaska, and multicentury basal area, leaf area index (LAI), and organic layer depth chronosequences measured in Saskatchewan, Manitoba, and Quebec. Collectively, these observations are diverse in terms of processes, time scales, and spatial extent. The second major objective is to use the updated model to understand how forest structure and soil carbon storage can be expected to change with increasing atmospheric CO_2, warming, and with changing nitrogen availability for different climates within the NA boreal forest.

Meeting these objectives will allow us to address the following questions. (1) Is it possible to accurately reproduce observed forest growth and soil organic layer dynamics along a climate gradient across the NA boreal forest by incorporating feedbacks between soil organic layer thickness and aboveground forest and

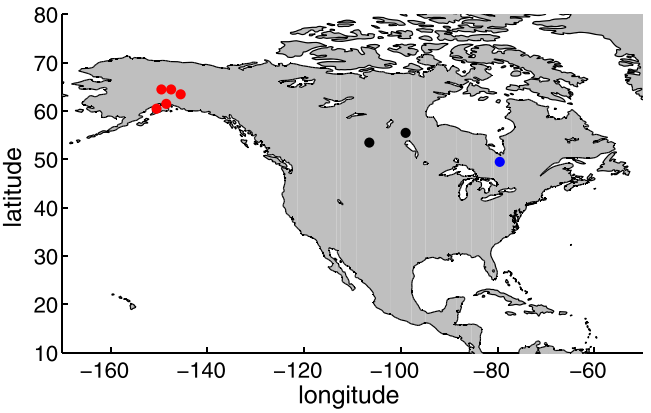

Figure 1. Map of model validation locations across the North American boreal forest. Validation measurements included (1) basal area measurements taken by the Cooperative Alaska Forest Inventory in multiple locations in central Alaska [*Malone et al.*, 2009], (2) net ecosystem productivity measurements taken using eddy flux towers near Delta Junction, Alaska [*Welp et al.*, 2007], (3) basal area, leaf area index, and soil organic matter chronosequences from Manitoba and Saskatchewan [*Bond-Lamberty et al.*, 2002b; *Harden et al.*, 2012], and (4) basal area and soil organic layer depth chronosequences from Quebec [*Fenton et al.*, 2005]. Different colors indicate different climate regimes in which the model was validated.

moss growth? (2) What are the effects of soil organic layer thickness on modeled forest composition and ecosystem carbon accumulation? How does the biological effect that the soil organic layer exerts on seedling and sucker recruitment compare to the physical effect of the soil organic layer on soil temperature and moisture, and hence organic matter decomposition? (3) How does global climate change, namely projected changes in atmospheric CO_2, temperature, and nitrogen availability, affect forest composition and ecosystem carbon accumulation and how do these changes vary across different climates within the NA boreal forest?.

2. Methods

2.1. Model Description

Our model simulations were carried out using ED2, a terrestrial biosphere model that explicitly scales up tree-level competition for light, water, and nutrients to the ecosystem level. Detailed descriptions of ED2 exist in the literature [*Medvigy and Moorcroft*, 2012; *Medvigy et al.*, 2009]. Single-grid cell simulations were carried out for the following three different climate regimes within the NA boreal forest to capture regional variability: (1) near Delta Junction, Alaska, where the mean January temperature is −19.2°C, the mean July temperature is 13.2°C, and the mean annual precipitation is 295 mm yr^{-1}; (2) near Thompson, Manitoba where the mean January temperature is −20.9°C, the mean July temperature is 18.2°C, and the mean annual precipitation is 509 mm yr^{-1}; and (3) in western Quebec where the mean January temperature is −17.3°C, the mean July temperature is 17.2°C, and mean annual precipitation is 905 mm yr^{-1} (Figure 1).

2.2. Experimental Overview

Our model experiments fell within two general categories, model evaluation and model sensitivity experiments. First, to evaluate our model's performance, we tested model simulations against observed net ecosystem productivity (NEP), basal area and leaf area growth, and soil organic matter accumulation. Second, we ran a series of experiments exploring the sensitivity of aspen-black spruce forest growth and carbon accumulation to environmental forcings that are projected to change with global climate change in the NA boreal forest. Each set of experiments was composed of an ensemble of simulations in order to capture the range of uncertainty associated with select ecophysiological parameters used in the model.

2.3. North American Boreal Ecosystem Dynamics in ED2

We have included the following newly developed parameterizations specific to the NA boreal forest into ED2: (1) aspen and black spruce functional types; (2) species-specific seedling growth dependent on organic layer depth; (3) species-specific litter decay rates; (4) a dynamic soil organic layer that includes dynamic moss growth with moss accumulation dependent on canopy tree type; and (5) an updated nitrogen cycle including mineralized soil nitrogen leaching due to soil water drainage and nitrogen fixation by cyanobacteria associated with moss. In addition, we include other recent developments, such as a new phenology scheme parameterized using NA boreal phenology observations of aspen [*Jeong and Medvigy*, 2014] and an updated plant hydraulics module [*Xu et al.*, 2016]. We refer to our updated model as "ED2-boreal." To our knowledge, no other terrestrial biosphere model applied to the large climate gradients within NA boreal forest couples dynamic NA boreal-specific vegetation with a dynamically accumulating soil organic layer and includes the species-specific effect of organic layer depth on seedling growth.

New aspen and black spruce plant functional types were parameterized by synthesizing measurements reported in previous studies (Table 1). Although our species choice of aspen and black spruce is not fully

Table 1. Ecophysiological and Life History Parameters for Aspen and Black Spruce

Parameter[a]	For Aspen	For Black Spruce	Unit	Reference
Allometric relation of diameter at breast height (dbh) to stem biomass[b]	b1 = 0.0255b2 = 2.844	b1 = 0.0404b2 = 2.658	kg C	Adapted from *Bond-Lamberty et al.* [2002a] and *Yarie et al.* [2007]
Allometric relation of dbh to tree height[c]	$h_{ref} = 0.2h_1 = -0.0776$	$h_{ref} = 0.5h_1 = -0.0631$	m	Adapted from *Bond-Lamberty et al.* [2002a] and *Yarie et al.* [2007]
Maximum tree height (h_{max})[c]	22.5	18.0	m	Adapted from *Bond-Lamberty et al.* [2002a] and *Yarie et al.* [2007]
Maximum rooting depth	1.0	0.3	m	*Strong and la Roi* [1983]
Specific leaf area	34.8	9.96	m^2 leaf $kg^{-1}C$	*Bond-Lamberty et al.* [2002b]
Specific root area	66.9	100.	m^2 root $kg^{-1}C$	*Steele et al.* [1997]
Ratio of fine roots to leaves	1.89	0.61	kg fine roots kg^{-1} leaves	*Ryan et al.* [1997]
Fine root turnover rate	0.65	1.56	yr^{-1}	*Pinno et al.* [2010] and *Ruess et al.* [2003]
Leaf turnover rate	End of growing season	0.14	yr^{-1}	*Hom and Oechel* [1983]
Density independent mortality	5.9×10^{-2}	1.4×10^{-2}	yr^{-1}	Adapted from *Bond-Lamberty et al.* [2014]
Sapwood area	0.62	0.45	Stem cross section fraction	*Yarie et al.* [2007]
Turgor loss point	−1.45	−4.35	MPa	*Way et al.* [2013] and *Abidine et al.* [1994]
Psi 50	−2.80	−4.26	MPa	*Sperry et al.* [1994] and *Balducci et al.* [2015]
Litter decomposition rate	1.8×10^{-4}	3.0×10^{-3}	d^{-1}	Adapted from *Euskirchen et al.* [2009] and *Prescott et al.* [2000]
Moss accumulation depth	a = 0	$a = 0.0043$; $b = -0.28$	cm	Equation (2) Based on *Fenton et al.* [2005]
Organic layer depth at which seedling mortality starts increasing (ol_min)	2.0	10.0	cm	Based on *Johnstone and Chapin* [2006a]
Organic layer depth at which seedling mortality stops increasing (ol_max)	5.0	40.0	cm	Based on *Johnstone and Chapin* [2006a] and *Fenton and Bergeron* [2006]
Background seedling mortality rate ($m_{p,min}$)	0.95	0.95	Fraction	Standard survivorship rate
Mortality shape parameter (c_1)	1.7	0.27		Fit to ol_min and ol_max
Treefall disturbance survivorship for trees smaller/larger than that 12 m	0.30/0.0	0.45/0.0	Fraction	*Rich et al.* [2007]
Carbon to nitrogen ratio for leaves and fine roots	33	63	Ratio	Adapted from *Bond-Lamberty et al.* [2006]
Nitrogen fixation Associated with moss biomass	0.0	$f = 7.73 \times 10^{-9}$	kg N d^{-1}	Adapted from nitrogen fixation data, Quebec clay belt, N. J. Fenton et al. (unpublished, 2015)
Moss bulk density		25 kg C m^{-2}		Adapted from *Trumbore and Harden* [1997] shallow organic layer bulk density
Litter bulk density	200 kg C m^{-2}	200 kg C m^{-2}		Adapted from *Trumbore and Harden* [1997] deep organic layer bulk density

[a]All other parameters are defined in Table 2 or we take as the default values for early successional hardwoods (aspen) and late successional conifers (black spruce) [*Medvigy et al.*, 2009].
[b]Based on biomass (b) to diameter at breast height (dbh) allometric equations of the form: $b = b1 \times dbh^{b2}$. Details can be found in *Medvigy et al.* [2009].
[c]Based on height (h) to diameter at breast height (dbh) allometric equations of the form: $h = h_{ref} + h_{max} \times [1 - \exp(h_1 \times dbh)]$. Details can be found in *Medvigy et al.* [2009].

representative of all NA boreal tree species, aspen and black spruce are some of the most abundant and widely distributed deciduous broadleaf and evergreen needleleaf species in the NA boreal forest. Aspen in particular is adept at growing in a diverse range of environmental conditions similar to those projected for the future NA boreal climate. An aspen-black spruce two species system has the advantage of simplicity and with it we hope to achieve a first order estimate of regional trends in forest composition and ecosystem carbon storage.

Previous sensitivity studies have identified that the maximum rate of carboxylation (V_{cmax}) and leaf biomass allometry exert particular control over the simulated dynamics [*Dietze et al.*, 2014; *White et al.*, 2000]. Substantial variation has been reported in field measurements of V_{cmax} for aspen and black spruce [*Kubiske et al.*, 1997; *Rayment et al.*, 2002]. However, models generally take a single value for V_{cmax} (at reference temperature) for each plant functional type. Under this construct, it is unclear how to capture the observed variability in V_{cmax} in terrestrial biosphere models. Likewise, the parameters linking leaf biomass to tree diameter can vary by location and tree size even for trees within the same species [*Ter-Mikaelian and Korzukhin*, 1997]. Our own preliminary analyses confirmed model sensitivity to these parameters. In addition, we also found that tree growth can be sensitive to the rate of nitrogen leaching, a parameter that is poorly

Table 2. Mean and Standard Deviation for the Prior Probability Density Functions for Select Ecophysiological and Hydrological Parameters

Parameter	For Aspen	For Black Spruce	Unit	Reference
Allometric relation of dbh to leaf biomass[a]	b1 = 0.0018 (2.1 × 10^{-4})[b]; b2 = 2.506	b1 = 0.033 (0.0033) [b]; b2 = 1.905	kg C	Adapted from *Bond-Lamberty et al.* [2002a] and *Yarie et al.* [2007]
Maximum photosynthetic capacity at 15°C	18.4 (1.6) [b]	8.07 (1.3)[b]	μmol m^{-2} s^{-1}	*Kubiske et al.* [1997] and *Rayment et al.* [2002]
Maximum seedling mortality rate ($m_{p,max}$)	1.0	0.9997 (0.0002)[b]	Fraction	Aspen from *Johnstone and Chapin* [2006a], black spruce adapted from [*Greene et al.*, 2004] and taking into account slow basal area decline in old (>500 year) black spruce forests
Soil nitrogen leaching efficiency	0.04 (0.015)[b]	0.04 (0.015)[b]	Fraction	Adapted from [*Gerber and Brookshire*, 2014]

[a]Based on biomass (b) to diameter at breast height (dbh) allometric equations of the form: $b = b1 \times dbh^{b2}$. Details can be found in [*Medvigy et al.*, 2009].
[b]Mean (standard deviation) of the normal prior probability density function defined to encompass the range of uncertainty of the parameter values. In the case of leaf biomass allometric coefficients, b2 was refit based on the value of b1. In the table, we only list the value of b2 corresponding to the mean parameter value used for b1.

constrained in terrestrial biosphere models. Finally, the upward bound of maximum seedling mortality fraction for black spruce in thick organic soils is poorly constrained [*Greene et al.*, 2004]. To account for these sources of parameter uncertainty, we defined normal priors representing a range of feasible parameter values. In the case of V_{cmax}, we used a range of values measured within a single study [*Kubiske et al.*, 1997; *Rayment et al.*, 2002]. Variations in leaf biomass allometry were derived from two site-specific allometric relations near Delta Junction, Alaska and Thompson Manitoba [*Bond-Lamberty et al.*, 2002a; *Yarie et al.*, 2007]. We derived the range in the rate of mineralized soil nitrogen leaching based on differences between parameterizations used by *Gerber and Brookshire* [2014] and the CLM model [*Oleson et al.*, 2010]. Finally, we placed uncertainty bounds on the maximum mortality fraction of black spruce seedlings based on our own sensitivity tests combined with millennial growth trends of old spruce forests [*Fenton et al.*, 2005] and germination measurements [*Greene et al.*, 2004]. The means and standard deviations of the priors for these parameters are reported in Table 2.

In our model, both aspen and black spruce experience increasing seedling mortality with increasing organic layer depth according to the following equation:

$$m_p = \max\left(\left(1-\exp\left(-c_1 \cdot OL_{depth}\right)\right) \cdot m_{p,\max},\ m_{p,\min}\right). \quad (1)$$

In equation (1), m_p is the seedling and sucker mortality fraction, $m_{p,max}$ is the species-specific maximum seedling and sucker mortality fraction in deep organic layers, c_1 is a positive species-specific shape parameter, OL_{depth} is the organic layer depth in centimeters, and $m_{p,min}$ is the background seedling and sucker mortality fraction characteristic of shallow organic layers (Tables 1 and 2). In ED2-boreal, aspen seedlings experience mortality rates greater than $m_{p,min}$ in organic layers thicker than 2 cm and 100% mortality in organic layers thicker than 5 cm in accordance with observations by *Johnstone and Chapin* [2006a]. In contrast, black spruce seedlings experience mortality rates greater than $m_{p,min}$ in organic layers thicker than 10 cm, and significantly elevated mortality in organic layers thicker than 40 cm [*Drobyshev et al.*, 2010; *Fenton and Bergeron*, 2006; *Fenton et al.*, 2006].

Greene et al. [2007] and *Lafleur et al.* [2015a] also find differential survivorship of aspen and black spruce seedlings in thick organic layers, although they reported different organic layer intervals over which mortality changes. Specifically, *Greene et al.* [2007] find that aspen seedling survivorship is 8000 times higher on an organic layer 0.5 cm than on one of 6 cm. In contrast, black spruce trees have a seedling survivorship ratio of 30 at these depths in absence of interspecies competition [*Greene et al.*, 2007]. *Lafleur et al.* [2015a] find that aspen seedling survivorship is relatively uninhibited in organic layers shallower than 10 cm, but seedling survivorship decreases linearly to 0% in organic layers greater than 25 cm [*Lafleur et al.*, 2015a]. Our uncertainty analysis of the maximum seedling mortality fraction for black spruce partially address this uncertainty in the literature.

For the purposes of this paper, we define fire severity in accordance with our parameterization of organic layer-induced seedling mortality. A severe fire is defined as any fire that reduces the soil organic layer to less than 4 cm, allowing regeneration of aspen seedlings. A moderate fire is defined as a fire event that reduces the soil organic layer to 4–40 cm such that aspen seedlings are unable to grow and black spruce

Table 3. Physical Properties of the Soil Organic Layer

Soil Organic Layer Property	Unit	Value
Soil moisture potential at saturation	m	−0.535
Soil moisture at saturation	$m^3\ m^{-3}$	0.469
Specific heat of dry soil	$J\ m^{-3}\ K^{-1}$	8.740×10^5
Hydraulic conductivity at saturation	$m\ s^{-1}$	2.358×10^{-6}
Soil field capacity	$m^3\ m^{-3}$	0.286
Wet soil albedo	Fraction	0.070
Dry soil albedo	Fraction	0.140
Bulk density	$kg\ m^{-3}$	500

seedlings grow with elevated mortality. Finally, we define a mild fire as any fire event with a residual soil organic layer greater than 40 cm, allowing very little regeneration of spruce seedlings [*Van Bogaert et al*., 2015]. All of our simulations are classified as developing after a mild, moderate, or severe burn, with the classification determined by the organic layer depth with which the simulation was initialized.

The model's surface litter inputs are composed of leaves, dead seeds, and black spruce fine roots. We assume that fine roots from aspen trees are present in the mineral soil and the structural tree litter is heterogeneously scattered on top of the soil organic layer, and so they are not included when calculating the organic layer depth. Litter loss occurs at a species-specific characteristic decay rate that is applied to an entire species' litter pool (leaves, fine roots, and seeds) as specified in Table 1. This characteristic rate is modified by temperature and moisture. The soil organic layer accumulates dynamically above the mineral soil and the soil organic layer depth is calculated as the sum of aspen litter (excluding fine roots), black spruce litter, and moss growth. Different bulk densities are assigned to the litter and moss pools due to the proximity of moss to the surface of the soil organic layer (Table 1) [*Carrasco et al*., 2006; *Trumbore and Harden*, 1997]. For the purposes of calculating temperature and water content, all components of the soil organic layer (both moss and litter) are assumed to have physical properties given in Table 3 [*McCumber and Pielke*, 1981]. Depending on thickness, the organic layer is discretized into one or more vertical layers so that gradients in temperature and soil moisture are resolved. Temperature and water content are calculated for each layer according to *Walko et al*. [2000].

Moss accumulation is observed in black spruce forests when the canopy begins to close and where deciduous leaf litter does not shade moss in the subcanopy [*Natalia et al*., 2008]. The net accumulation rate has been found to be mainly a function of forest age and canopy species-type such that moss is present in black spruce forests but not aspen forests [*Zackrisson et al*., 2004]. Here we model net moss biomass accumulation using the following equation:

$$\frac{ds}{dt} = \begin{cases} a \cdot s^b, l_a < 0.05 \\ 0, l_a \geq 0.05 \end{cases}. \tag{2}$$

In equation (2), s is moss biomass in $kg\ C\ m^{-2}$, dt is a monthly time step, and l_a is the amount of aspen litter present in $kg\ C\ m^{-2}$. We set a threshold for moss growth of 0.05 $kg\ C\ m^{-2}$ of aspen litter, above which moss does not accumulate, preventing moss growth in aspen-dominated stands. We parameterized the constants a and b using a percent *Sphagnum* moss cover chronosequence measured in the Abitibi clay belt region of Quebec [*Fenton et al*., 2005]. Similar to *Bona et al*. [2016], in our analysis we found *Sphagnum* percent cover to be proportional to moss biomass in chronosequence points with ^{14}C ages younger than 750 years. With this parameterization, net moss accumulation is dependent only on aspen litter and previous month's moss biomass; it is not affected by changes in the temperature or moisture regime. In ED2-boreal, moss biomass is included as part of the soil organic layer for the purposes of calculating seedling survivorship, resolving the soil energy and water balance and calculating total ecosystem carbon.

In the updated nitrogen cycle in ED2-boreal, when a tree dies or sheds its fine roots, needles, or leaves, both the aboveground carbon and nitrogen pools are transferred to the soil system. Soil organic matter decomposition rate is modified by species litter type, soil temperature, and soil moisture [*Moorcroft et al*., 2001]. As carbon is mineralized, the associated nitrogen from the decomposing structure is released into a bioavailable mineralized soil nitrogen pool. Each day, tree demand for nitrogen is calculated and the amount of nitrogen removed from the bioavailable soil nitrogen pool is the minimum of either the soil

nitrogen available to the plant or the nitrogen required for growth. Any remaining mineralized soil nitrogen after plant nitrogen uptake is subjected to leaching loss with the assumption that a small fraction (see Table 2) is in soluble form and loss occur as a function of soil water drainage out of the rooting zone [*Thornton and Rosenbloom*, 2005]. Additional mineralized soil nitrogen inputs include atmospheric nitrogen deposition and, in older spruce forests, nitrogen fixation by cyanobacteria associated with *Sphagnum* moss. Here we model nitrogen fixation as increasing with the amount of *Sphagnum* moss according to the following relationship:

$$N_{fix} = \begin{cases} f \cdot s, s \geq 2.5 \\ 0, s < 2.5 \end{cases}. \quad (3)$$

In equation (3), N_{fix} is the nitrogen fixation rate in kg N d^{-1} and f is a constant. When moss biomass accumulates to approximately 2.5 kg C m^{-2}, an increasing presence of *Sphagnum* moss that associates with nitrogen-fixing cyanobacteria results in a linear increase in nitrogen fixation with moss biomass (N. J. Fenton et al., unpublished data, 2015). Because in this study we focus on forest recovery from fire and do not include dynamic fire disturbance, we do not specifically address how combustion losses affect the long-term mass balance of forest nitrogen. Postfire nitrogen fertilization depends on the fire severity scenario and the nitrogen available in the residual soil organic layer.

2.4. Model Evaluation

We assessed whether our model could accurately simulate aspen and black spruce forest growth and soil organic layer accumulation over long-time scales in addition to capturing monthly net ecosystem productivity (NEP). For this assessment, we utilized observations that varied with respect to both measurement type and measurement location in order to scale up to different climate regimes within the NA boreal forest (Figure 1). None of the observations used to evaluate the model performance were used during model calibration. To our knowledge, no previous studies have challenged models in the NA boreal zone with such diverse observations in terms of time scale, measurement type, and range of climate gradients. Unless otherwise specified, all of our simulations were forced with 1.0°, 3 hourly meteorology from the Princeton Global Forcing (PGF) data set [*Sheffield et al*., 2006], atmospheric CO_2 levels were held constant at 370 ppm, and nitrogen deposition rates were held constant at 0.5 g N m^{-2} yr^{-1} for simulations in Canada and 0.1 g N m^{-2} yr^{-1} for simulations in Alaska [*Reay et al*., 2008].

Each model evaluation was composed of a 20 member ensemble of simulations that captured the range of uncertainty associated with select ecophysiological parameters used in the model (Table 2). In a preliminary analysis, we tested ensemble sizes ranging from 1 to 30 and determined that the ensemble mean and standard deviation stabilized at around 15–20 members. Each ensemble member was initialized with a random draw from the joint prior probability distribution for V_{cmax}, leaf allometry, maximum seedling mortality fraction, and soil nitrogen leaching rate. The same 20 parameter sets were used in all of our analyses. Additional details on simulations and model evaluations are available in Table 4.

To assess our model's ability to reproduce monthly NEP in both aspen and black spruce forests, we compared two 3 year (2002–2004) eddy covariance records from an aspen and black spruce forests situated near Delta Junction, Alaska [*Welp et al*., 2007] to simulated NEP for the same locations. Inventory data were not available at the sites so we carried out preliminary spin-up runs to initialize the model forest cover so that modeled leaf area index (LAI) was similar to that of the observed forest LAI during the measurement years [*Liu et al*., 2005]. Each model forest was grown from a seedling density of 0.2 m^{-2}. For the model spin-up, we used PGF meteorology looped over years 2002–2004. The aspen forest soil organic layer was initialized to 3 cm in depth (typical of a secondary successional aspen forest in Alaska). The black spruce forest was initialized with a 15 cm soil organic layer (a typical organic layer that would allow black spruce trees to be the primary species growing during secondary succession). Both forests were grown on a mineral soil of silty clay loam texture according to observations. Following the spin-up, we compared simulated and observed NEP. To assess performance, we computed the ensemble mean and percent error between ensemble mean and observations for each month in the growing season (May–August).

To validate ED2-boreal for decadal-scale forest growth in Alaska, we compared successive forest inventories from Cooperative Alaska Forest Inventory (CAFI) [*Malone et al*., 2009] with simulated forest growth. First, we grouped inventory plots based on their composition (pure aspen, pure black spruce, mixed aspen-black

Table 4. Model Validation Experiments

Simulation Name (Subject[a])-(Type[b])-(Location)	Location (lat/lon)	Observational Data Set (Reference)	Simulation Summary
BS-chrono-MB	55.5/−98.5	BOREAS Northern Study Area dry chronosequence [*Bond-Lamberty et al.*, 2002b]	0.2 m^{-2} black spruce seedling density; initial organic layer depth = 15 cm; looped over 1990–2008 meteorology and CO_2 = 370 ppm; nitrogen deposition rate = 0.5 g N m^{-2} yr^{-1}
TA-chrono-MB	55.5/−98.5	BOREAS Northern Study Area old aspen forest	0.2 m^{-2} aspen seedling density; initial organic layer depth = 3 cm; looped over 1990–2008 meteorology and CO_2 = 370 ppm; nitrogen deposition rate = 0.5 g N m^{-2} yr^{-1}
BS-chrono-SK	53.5/−104.5	BOREAS Southern Study Area old black spruce forest	0.2 m^{-2} black spruce seedling density; initial organic layer depth = 15 cm; looped over 1990–2008 meteorology and CO_2 = 370 ppm; nitrogen deposition rate = 0.5 g N m^{-2} yr^{-1}
TA-chrono-SK	53.5/−104.5	BOREAS Southern Study Area old aspen forest	0.2 m^{-2} aspen seedling density; initial organic layer depth = 3 cm; looped over 1990–2008 meteorology and CO_2 = 370 ppm; nitrogen deposition rate = 0.5 g N m^{-2} yr^{-1}
BS-mod-chrono-QC	49.0/−79.0	Moderately burned black spruce and organic layer depth chronosequence, [*Fenton et al.*, 2005]	0.2 m^{-2} black spruce seedling density; initial organic layer depth = 20 cm; looped over 1990–2008 meteorology and CO_2 = 370 ppm; nitrogen deposition rate = 0.5 g N m^{-2} yr^{-1}
BS-mild-chrono-QC	49.0/−79.0	Mildly burned black spruce and organic layer depth chronosequence, [*Fenton et al.*, 2005]	0.2 m^{-2} black spruce seedling density; initial organic layer depth = 45 cm; looped over 1990–2008 meteorology and CO_2 = 370 ppm; nitrogen deposition rate = 0.5 g N m^{-2} yr^{-1}
BS-north-CAFI-AK	65.0/−148.0	Cooperative Alaska Forest Inventory [*Malone et al.*, 2009]	5 years (two inventories), six sites, 2002–2007 meteorology
BS-south-CAFI-AK	61.0/−151.0	Cooperative Alaska Forest Inventory [*Malone et al.*, 2009]	10 years (three inventories), six sites, 2002–2012 meteorology
TA-north-CAFI-AK	65.0/−150.0	Cooperative Alaska Forest Inventory [*Malone et al.*, 2009]	5 years, (two inventories), four sites, 1995–2000 meteorology
TA-south-CAFI-AK	62.0/−149.0	Cooperative Alaska Forest Inventory [*Malone et al.*, 2009]	10 years (three inventories), five sites, 2001–2011 meteorology
Mixed-CAFI-AK	60.0/−150.0	Cooperative Alaska Forest Inventory [*Malone et al.*, 2009]	10 years (three inventories), three sites, 2003–2012 meteorology
TA-EC-AK	63.5/−145.5	Eddy Flux measurements near Delta Junction, AK [*Welp et al.*, 2007]	Spin up with 0.2 m^{-2} aspen seedling density and a 3 cm organic layer. Compared simulation year with similar LAI [*Liu et al.*, 2005] and 2002–2004 meteorology
BS-EC-AK	63.5/−145.5	Eddy Flux measurements near Delta Junction, AK [*Welp et al.*, 2007]	Spin up with 0.2 m^{-2} black spruce seedling density and a 15 cm organic layer. Compared simulation year with similar LAI [*Liu et al.*, 2005] and 2002–2004 meteorology

[a]Black spruce (BS); aspen (TA); and mixed aspen and black spruce forest (mixed).
[b]Chronosequence (chrono); Cooperative Alaska Forest Inventory (CAFI); eddy covariance (EC).

spruce) and location (northern or southern) so that we could assess model performance in both monoculture and mixed stands along a climate gradient within interior Alaska. The grouping by climate was determined based on the 1° PGF meteorology. Grid boxes associated with each grouping are detailed in Table 4. This grouping resulted in five categories of simulations: northern and southern simulations initialized with pure aspen (TA-north-CAFI-AK; TA-south-CAFI-AK), northern and southern simulations initialized with pure black spruce (BS-north-CAFI-AK; BS-south-CAFI-AK), and a southern simulation initialized with mixed forest (Mixed-CAFI-AK). The CAFI did not include any mixed stands in the northern region. Three to six inventory plots were present within each category, and each plot was simulated separately with a 20 member ensemble.

Because ED2-boreal tracks the size and density of cohorts of trees, it is possible to initialize ED2-boreal with inventory data of tree diameter at breast height (DBH) and soil carbon from CAFI. Nitrogen data were not available, so we initialized the soil nitrogen as proportional to basal area in forests with aspen and inversely proportional to the basal area in forests with only black spruce [*Jerabkova et al.*, 2006]. Each plot was initialized with a mineral soil of silty clay loam texture. In our assessment of model performance, we calculated average percent error in basal area between the observed and simulated category mean.

We also validated ED2-boreal with basal area, LAI, and soil carbon chronosequences for aspen forests and black spruce forests in locations in Saskatchewan and Manitoba measured as part of the BOREAS campaign [*Sellers et al.*, 1997]. In the BOREAS Northern Study Area (NSA) in Manitoba, we compared simulated forest growth to the dry black spruce chronosequence and the old aspen forest [*Bond-Lamberty et al.*, 2002b] and we compared the simulated soil carbon accumulation in black spruce forests after 150 years to observed

carbon storage in shallow organics [*Harden et al*., 2012]. In Southern Study Area (SSA) in Saskatchewan, we compared simulated forest growth to both the old aspen and black spruce forests. This evaluation involved four sets of 20 ensembles members each: one set for an aspen-only seeded forest (TA-chrono-MB) and one set for a black spruce-only seeded forest (BS-chrono-MB) at the NSA, and one set for an aspen-only seeded forest (TA-chrono-SK) and one set for a black spruce-only seeded forest (BS-chrono-SK) at the SSA. Each black spruce and aspen forest was spun-up from seedlings at a density of 0.2 m^{-2}. The aspen forest soil organic layer was initialized to 3 cm in depth and the black spruce forest was initialized with a 15 cm thick soil organic layer. Forests were grown on a mineral soil of clay texture according to observations. Simulations were forced with PGF meteorology looped over years 1990–2008. We assessed model performance by computing the ensemble mean and percent error between simulated mean and measured basal area and LAI.

Several factors complicate comparison of simulated forest growth to chronosequences. Each point measured in a forest chronosequence grew under different atmospheric CO_2 conditions and under a different climate forcing, depending on the age of the chronosequence point. To determine whether this was important for our analysis, we performed separate model simulations for each chronosequence point, forcing the model with dynamic atmospheric CO_2 corresponding to the levels seen by each forest throughout its lifetime. From these tests, we found that the forest adjustment to increasing atmospheric CO_2 is sufficiently rapid that it is unnecessary to include separate simulations for each chronosequence point. We also found that the overall growth trends of the forest were not very sensitive to the interval over which we looped the meteorology, provided that the interval was longer than 5 years and was not composed mainly of anomalous years.

In the eastern NA boreal forest, we compared our model simulations to two black spruce basal area and organic layer depth chronosequences measured after a moderate fire disturbance and a mild fire disturbance in the Clay Belt region of Quebec [*Fenton et al*., 2005]. Accurately capturing differing growth dynamics of black spruce in diverse initial conditions is particularly important in eastern Canada because the fire return interval is long, old black spruce forests of multiple generations are common, and the structure of the forest changes significantly as the forest ages and the soil organic layer accumulates [*Bergeron and Fenton*, 2012]. We limit the scope of our analysis to the ^{14}C-dated forest age and chronosequence points less than 500 years old. The current fire cycle in eastern Canada is approximately 500 years, and the long-term average was previously around 140 years, ensuring that the majority of stands present in this region are younger than 500 years [*Bergeron et al*., 2004]. Each evaluation was composed of 20 ensemble members with meteorology looped over years 1990–2008 and stands initialized with a seedling density of 0.2 m^{-2}. The soil organic layer was initialized to 20 cm with no moss present in the moderate burn simulation (BS-mod-chrono-QC). The mild burn simulation (BS-mild-chrono-QC) was initialized with a 45 cm soil organic layer composed of litter and moss. Forests were grown on a mineral soil of clay texture according to observations.

2.5. Model Experiments

We performed five sensitivity experiments exploring the sensitivity of forest composition and ecosystem carbon accumulation to changes in organic layer conditions and increased temperature, nitrogen availability, and atmospheric CO_2. The motivation for these experiments was twofold. First, changes in fire regime and increases in temperature, nitrogen deposition, and atmospheric CO_2 are likely to happen over the next century. Second, both increases in temperature and changes in nitrogen are directly linked to NA boreal forest soil organic matter accumulation; the soil organic layer accumulation rate is highly dependent on temperature-regulated decomposition and the rate of organic matter decomposition directly controls the rate of nitrogen cycling. Though whole-plant response to increases in atmospheric CO_2 is poorly understood [*Nowak et al*., 2004], NA boreal forest carbon accumulation rates may be increasing in response to increasing atmospheric CO_2 and could potentially store CO_2 in plant biomass or soil organic matter, at least in the proximate future [*Trumbore and Harden*, 1997]. As such, leaf-level carbon assimilation rates calculated by ED2-boreal could be used as an upper bound for the carbon drawdown sensitivity of the NA boreal forest under elevated atmospheric CO_2. Changes in precipitation were not included in our simulations because climate models give conflicting projections [*Allen and Ingram*, 2002]. Because our simulations do not include changes in the full set of environmental forcings, they should be viewed as sensitivity studies rather than future projections.

Table 5. Model Experiments

Simulation Name	Duration (Years)	Experiment
Burn-mild	500	Initial organic layer depth 60 cm
Burn-severe	500	Initial organic layer depth 3 cm
OLon-SMon	300	Initial organic layer depth 60 cm, organic layer-dependent seedling mortality module on, dynamic soil organic layer on
OLon-SMoff	300	Initial organic layer depth 60 cm, organic layer-dependent seedling mortality module off, dynamic soil organic layer on
OLoff-SMoff	300	Initial organic layer depth 60 cm, organic layer-dependent seedling mortality module off, dynamic soil organic layer off
OLon-SMon-warm	300	Initial organic layer depth 60 cm, organic layer-dependent seedling mortality module on, dynamic soil organic layer on, 4°C mean annual temperature increase, conserve relative humidity
OLon-SMoff-warm	300	Initial organic layer depth 60 cm, organic layer-dependent seedling mortality module off, dynamic soil organic layer on, 4°C mean annual temperature increase, conserve relative humidity
OLoff-SMoff-warm	300	Initial organic layer depth 60 cm, organic layer-dependent seedling mortality module off, dynamic soil organic layer off, 4°C mean annual temperature increase, conserve relative humidity
T-0Cwarm	300	Initial organic layer depth 3 cm (60 cm in QC), current meteorological forcing
T-2Cwarm	300	Initial organic layer depth 3 cm (60 cm in QC), 2°C mean annual temperature increase, conserve relative humidity
T-4Cwarm	300	Initial organic layer depth 3 cm (60 cm in QC), 4°C mean annual temperature increase, conserve relative humidity
Ndep-0.1	300	Initial organic layer depth 3 cm, nitrogen deposition 0.1 gN m^{-2} yr^{-1}
Ndep-0.5	300	Initial organic layer depth 3 cm, nitrogen deposition 0.5 gN m^{-2} yr^{-1}
Ndep-2	300	Initial organic layer depth 3 cm, nitrogen deposition 2 gN m^{-2} yr^{-1}
Ndep-20	300	Initial organic layer depth 3 cm, nitrogen deposition 20 gN m^{-2} yr^{-1}
CO2-370	300	Atmospheric CO_2 370 ppm, initial organic layer depth 3 cm (60 cm in QC),
CO2-1000	300	Atmospheric CO_2 1000 ppm, initial organic layer depth 3 cm (60 cm in QC),

In our sensitivity experiments, the 20 ensemble members used the same 20 parameter sets as in the model evaluations. Each experiment included ensembles of a hypothetical mixed aspen and black spruce forests simulated with the climate of Delta Junction, Alaska; Thompson, Manitoba; and in the Abitibi, on the Clay Belt of Quebec and Ontario. This spatial distribution was designed so that we could (1) identify the unifying processes occurring throughout the NA boreal forest and (2) resolve the differing regional responses due to a climate gradient. All ensembles were initialized with aspen and black spruce seedlings, each at a density of 0.2 m^{-2} and were forced with meteorology looped over years 1990–2008. We assessed (1) the effect of fire severity, (2) the biological and physical effect of the soil organic layer, (3) the effect of projected mean annual temperature increases, (4) the effect of projected changes in nitrogen deposition, and (5) the effect of projected increases in atmospheric CO_2 on forest composition and total ecosystem carbon accumulation. In our experiments, total ecosystem carbon was computed as the sum of plant carbon, coarse woody debris carbon, dead seeds, discarded fine roots, discarded leaves, and moss carbon. Forest composition was assessed based on the ratio of aspen biomass to total tree biomass (aspen plus black spruce). Simulations are described in detail below and summarized in Table 5.

To examine the effect of fire severity on forest composition and total ecosystem carbon accumulation, we ran two sets of 500 year ensembles for each site along the regional climate gradient, one representing forest development after a severe fire where the soil organic layer was mostly burned (burn-severe) and one representing forest development after a mild fire (burn-mild) where a thick organic layer remained (Table 5).

To disentangle the biological and physical effects of the soil organic layer, we ran six sets of 300 year ensembles. The first ensemble corresponds to the standard ED2-boreal configuration in which the dynamic organic layer and seedling mortality module are active (OLon-SMon). For the second ensemble, the dependence of seedling mortality on organic layer depth was turned off (OLon-SMoff). For the third ensemble, both the dependence of seedling mortality on organic layer depth and the dynamic organic layer were turned off (OLoff-SMoff). Our next three experiments (OLon-SMon-warm, OLon-SMoff-warm, OLoff-SMoff-warm) replicated the first three experiments but also included with a uniform increase in temperature of 4°C to isolate possible changes in the biological and physical effects of the soil organic layer with warming temperature. Other meteorology, including precipitation, solar radiation, and relative humidity, were not

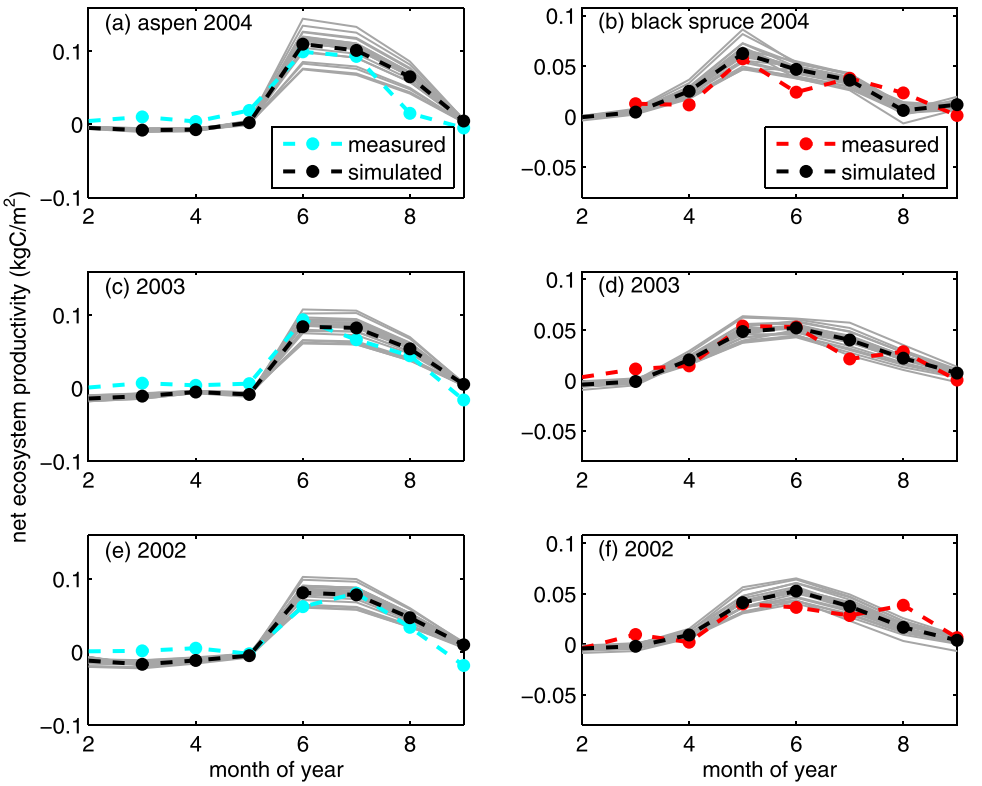

Figure 2. Comparison of simulated and observed net ecosystem productivity (NEP) of aspen and black spruce forests in central Alaska. Simulated ensemble members (grey) and ensemble mean (black) of the monthly sum of NEP shown with the measured monthly sum of NEP for an aspen (blue) and black spruce (red) forests near Delta Junction, Alaska for years 2002–2004. Limited quality-controlled observational data were available October through January, so these data points were omitted.

changed. All ensembles were initialized as if developing after a mild fire disturbance with an organic layer depth of 60 cm (Table 5). The initial organic layer depth was chosen to highlight conditions in which including the seedling mortality module and dynamic soil organic layer would most affect the outcome of forest composition and total ecosystem carbon accumulation.

In our third set of experiments, to examine the effect of warming temperatures, ensembles were forced with current meteorological conditions (T-0Cwarm), with a uniform increase in temperature of 2°C (T-2Cwarm), and with a uniform increase in temperature of 4°C (T-4Cwarm). Other meteorology, including precipitation, solar radiation, and relative humidity, were unchanged. Forests in these simulations were initialized to represent stand development after fire disturbance in the upcoming century near Delta Junction, Alaska, Thompson, Manitoba, and the Clay Belt of Quebec. Fire severity is projected to increase in both Manitoba and Alaska in the upcoming century [*Girardin et al*., 2013; *Hinzman et al*., 2013; *Kasischke and Turetsky*, 2006]; however, in the Clay Belt in Quebec, fire severity is not projected to increase leading up to year 2100 [*Terrier et al*., 2014]. Thus, we initialized the forests in Alaska and Manitoba with a thin organic layer of 3 cm and the forest in Quebec with a thick organic layer of 60 cm.

In our fourth set of experiments, we examined the effect of changes in nitrogen with four different nitrogen deposition scenarios for all locations: annual nitrogen deposition rates of (1) 0.1 g N m^{-2} yr^{-1}, comparable to deposition rates currently seen in Alaska (Ndep-0.1); (2) 0.5 g N m^{-2} yr^{-1}, comparable to rates seen in many parts of Canada (Ndep-0.5); (3) 2 g N m^{-2} yr^{-1}, projected for the year 2030 in some areas in southern Quebec (Ndep-2) [*Reay et al*., 2008]; and (4) 20 g N m^{-2} yr^{-1} (Ndep-20). All simulations were initialized to represent stand development after fire disturbance in the upcoming century near Delta Junction, Alaska, Thompson, Manitoba, and the Clay Belt of Quebec (Table 5).

In our final set of experiments, we examined the effect of atmospheric CO_2 fertilization. In ED2-boreal, the effect of atmospheric CO_2 fertilization on leaf-level carbon assimilation and water fluxes is computed using the model developed by Farquhar, Ball, Berry and others, described in detail in Appendix B of *Medvigy et al*.

[2009]. We ran two sets of 300 year ensembles with atmospheric CO_2 fixed at 370 ppm (CO2-370) and with atmospheric CO_2 fixed at 1000 ppm (CO2-1000), a high-emissions scenario for the year 2100 [*IPCC*, 2013]. Meteorology including temperature, precipitation, solar radiation, and relative humidity were unchanged. All simulations were initialized to represent stand development after a fire disturbance in the upcoming century near Delta Junction, Alaska, Thompson, Manitoba, and the Clay Belt of Quebec (Table 5).

3. Results

3.1. Model-Data Comparison

When compared to measured NEP near Delta Junction, Alaska, the simulated ensemble mean captured the seasonal and interannual trends for both aspen (Figures 2a, 2c, 2e) and black spruce (Figures 2b, 2d, 2f) forests for years 2002–2004. In the aspen forest, both simulated and observed total growing season (May–August) NEP increased each year between 2002 and 2004. In the black spruce forest, total growing season NEP increased between 2002 and 2003 and decreased between 2003 and 2004. This initial increase in growing season NEP followed by a decline in 2004 was also captured in the model simulations. We found that the model best reproduced carbon fluxes in the aspen forest in June and July, where the simulated ensemble mean was within 17.5% of the observed NEP (Figures 2c, 2e, and Table 6). In May, the absolute difference between observed and simulated ensemble-mean NEP was not large, but the small denominator in the percent error calculation resulted in a large percent error (Figures 2a, 2c, 2e, and Table 6). The poor performance of the model in the aspen forest in August was caused by a discrepancy between observed and simulated NEP in 2004 (Figure 2a). During 2004, a major drought occurred in central Alaska, so it is possible that the simulated NEP was not as sensitive to the drought conditions. In contrast, the simulated NEP at the

Table 6. Error Statistics for Model Runs

Observational Dataset	Mean Percent Error[a]	Ensemble Range[b]	Units
BOREAS NSA dry black spruce basal area chronosequence	26.2	16.1/36.7	$m^2\ ha^{-1}$
BOREAS NSA dry black spruce LAI chronosequence	4.5	2.5/4.7	$m^2\ m^{-2}$
BOREAS NSA old aspen forest basal area	0.4	4.9/35.1	$m^2\ ha^{-1}$
BOREAS NSA old aspen forest LAI	21.3	0.5/3.7	$m^2\ m^{-2}$
BOREAS SSA old black spruce forest basal area	4.2	18.0/37.8	$m^2\ ha^{-1}$
BOREAS SSA old aspen forest basal area	0.7	27.8/36.7	$m^2\ ha^{-1}$
BOREAS SSA old aspen forest LAI	1.5	2.6/3.5	$m^2\ m^{-2}$
Quebec moderately burned black spruce basal areachronosequence	40.4	6.0/45.4	$m^2\ ha^{-1}$
Quebec moderately burned organic layer depthchronosequence	17.6	40.2/53.0	Cm
Quebec mildly burned black spruce basal area chronosequence	31.9	4.1/39.0	$m^2\ ha^{-1}$
Quebec mildly burned organic layer depth chronosequence	9.7	46.7/53.6	cm
CAFI northern black spruce forest basal area inventory	4.5	4.0/26.9	$m^2\ ha^{-1}$
CAFI southern black spruce forest basal area inventory	5.4	11.0/19.8	$m^2\ ha^{-1}$
CAFI northern aspen forest basal area inventory	0.3	16.8/28.4	$m^2\ ha^{-1}$
CAFI southern aspen forest basal area inventory	9.1	13.5/24.5	$m^2\ ha^{-1}$
CAFI; mixed stand black spruce basal area inventory	45.3	3.9/26.9	$m^2\ ha^{-1}$
CAFI; mixed stand aspen basal area inventory	3.1	9.5/24.5	$m^2\ ha^{-1}$
Aspen forest eddy flux measurements near Delta Junction, AK	57.4 (72.4/17.3/12.1/127.8)[c]	−8.2/−1.8 66/120 62/120 40/760	$gC\ m^{-2}$
Black spruce forest eddy flux measurements near Delta Junction, AK	29.2 (7.7/17.8/22.8/68.7)[c]	40/71 41/59 25/53 4.7/28	$gC\ m^{-2}$

[a]For the chronosequences, the point-wise mean percent error was calculated using ensemble mean and observational mean at all chronosequence points. The mean percent error was calculated as the average of the point-wise mean percent errors. For the forest inventory, the mean percent error was calculated using combined group and ensemble means and the group observational mean at a given return inventory. We then averaged the percent error over all return inventories at a given site. For the eddy covariance data, the mean percent error was calculated using ensemble mean averaged over 2002–2004 for each month in the growing season (May/June/July/August) and the observational mean averaged over 2002–2004 for each month in the growing season. We also computed mean percent error for the entire growing season.

[b]Ensemble range indicates the simulated minimum/maximum ensemble members at the latest chronosequence point or forest inventory. For the eddy covariance data, we computed the average maximum and average minimum over each growing season month (May–August) for 2002–2004.

[c]The first number represents the mean present error for the entire growing season. We separated out mean percent error by month (May/June/July/August) in the parentheses.

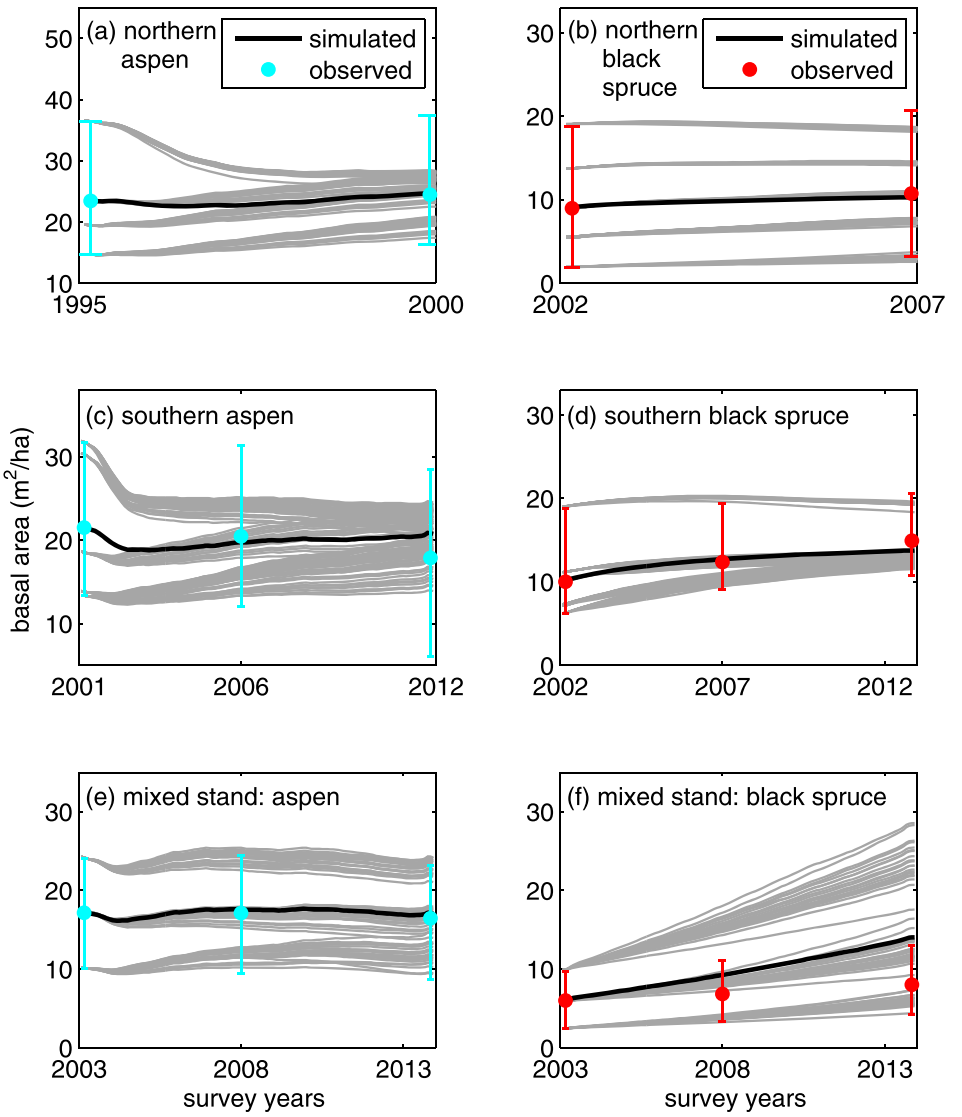

Figure 3. Comparison of simulated and observed basal area growth for aspen, black spruce, and mixed forests at forest inventory sites in central Alaska. Simulated forest basal area of the combined group and ensemble means (black) and group and ensemble spread (grey) are shown with the observed mean and range for five different groups of inventories in the Alaskan boreal forest. We initialized the model with the first inventory at each site. The initial spread at the first inventory between different groups of ensembles was due to variations in basal area between the different sites within the same group. We next compared successive forest inventories with the simulated group and ensemble mean of forest growth for groups of northern (a) and southern (c) aspen forests, groups of northern (b) and southern (d) black spruce forests, as well as a group of mixed aspen (e) and black spruce (f) forests.

black spruce forest did respond to the drought conditions of 2004 with a dip in NEP that was more pronounced than in the observations (Figure 2b). For all growing season months except for August, the ensemble mean for the black spruce forest was within 23% of the observed NEP. However, in August, the ensemble mean underpredicted NEP relative to the observations by 69% (Figures 2b, 2d, 2f, and Table 6).

We found that the model was able to capture patterns in forest basal area growth when compared to the CAFI across a climate gradient within central Alaska (Figure 3). For aspen trees in both monoculture and mixed stand categories, the combined ensemble and category mean came within 10% of the observed category mean basal area growth and the range in simulated basal area fell within the range of observations (Table 6 and Figures 3a, 3c, 3e). In the black spruce monocultures, the combined ensemble and category mean came within 5.5% of the observed category mean and the simulated range in basal area generated by the different ensembles was nearly identical to the CAFI range (Figures 3b, 3d, and Table 6). However, in

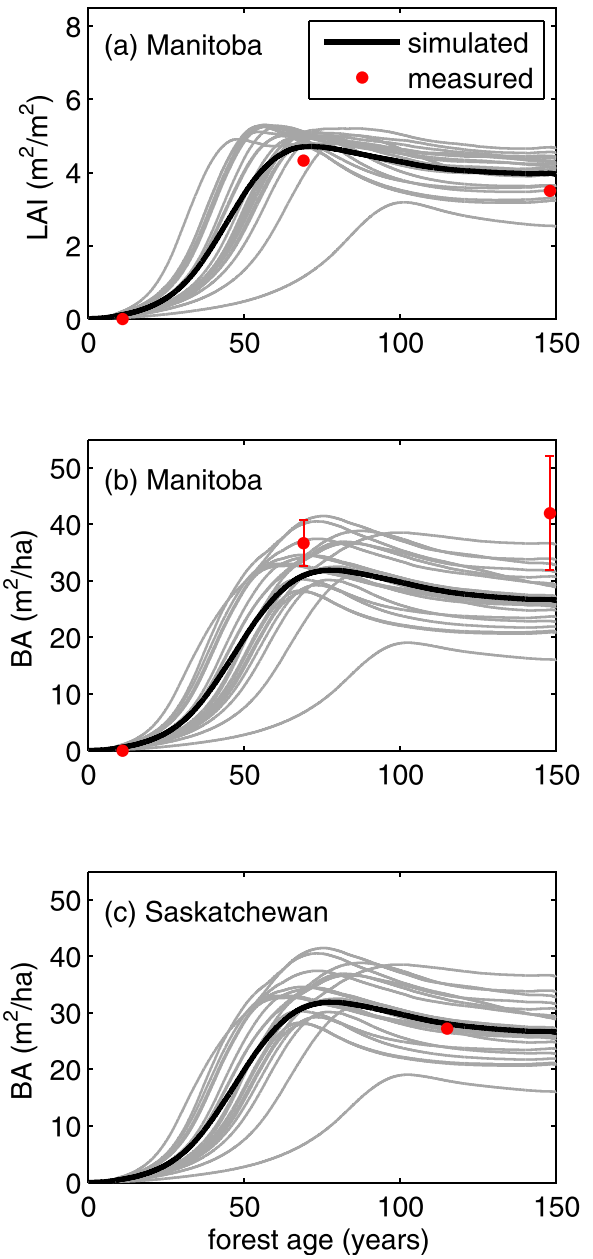

Figure 4. Comparison of simulated and observed black spruce basal area (BA) and leaf area index (LAI) growth in central Canada. For BA and LAI, simulated ensemble members are indicated in grey, the ensemble mean is indicated in black, and measured forest chronosequence points are indicated in red. Error bars, available for only a subset of the observations, indicate the upper and lower decile bounds of the observations. Measurements of LAI and BA were taken in the BOREAS Northern Study Area near Thompson, Manitoba (a-b) and the BOREAS Southern Study Area near Prince Albert (c).

the mixed stand category, the model overpredicted black spruce basal area growth by an average of 45.3% (Table 6 and Figure 3f).

When compared to the century-long chronosequences in central Canada, the simulated ensemble mean captured initial forest growth and maximum basal area and LAI for both black spruce and aspen forests (Figures 4 and 5). In the black spruce forests near Thompson Manitoba, the average percent error between the simulated ensemble mean and measured LAI and basal area was 4.5% and 26%, respectively (Figures 4a, 4b, and Table 6). In this particular simulation set, the maximum black spruce forest basal area was controlled by the nitrogen availability and ensemble members with a lower nitrogen leaching efficiency simulated forest basal area values within 13% of the observations (Figure 4b). After 150 years, we found that the simulated spruce forests accumulated an average of 5.36 kg C m^{-2} in the soil organic layer, well within the observed range of ~1.8–12 kg C m^{-2} [*Harden et al*., 2012]. In Saskatchewan, the average percent error between the simulated ensemble mean and observed basal area in the old black spruce forest was 4.2% (Figure 4c and Table 6). In the 53 year-old aspen forest in Manitoba, the simulated ensemble mean came within 0.4% and 21.2% of the observed basal area and LAI, respectively (Figures 5a, 5b, and Table 6). Finally, in the 67 year-old aspen forest in Saskatchewan, the simulated ensemble mean came within 0.7% and 1.5% of the observed basal area and LAI, respectively (Figures 5c, 5d, and Table 6).

In the Clay Belt region of Quebec, the model was able to reproduce the distinct growth response of black spruce in different fire disturbance scenarios (Figure 6). Here, the difference in simulated forest growth was due mainly to changes in spruce seedling establishment. In the mild burn chronosequence (Figures 6a and 6b), the average percent error between the simulated ensemble mean and observed basal area and organic layer thickness was 32% and 10%, respectively (Figures 6a, 6b, and Table 6). The ensemble mean and almost all of the ensemble members fell well within the upper and lower decile bounds of the observed basal area (Figure 6a) and all ensemble members fell within the bounds of observed organic layer depths (Figure 6b).

In the moderately burned Quebec chronosequence, the average percent error between the simulated ensemble mean and observed basal area and organic layer thickness was 40.4% and 17.5%, respectively.

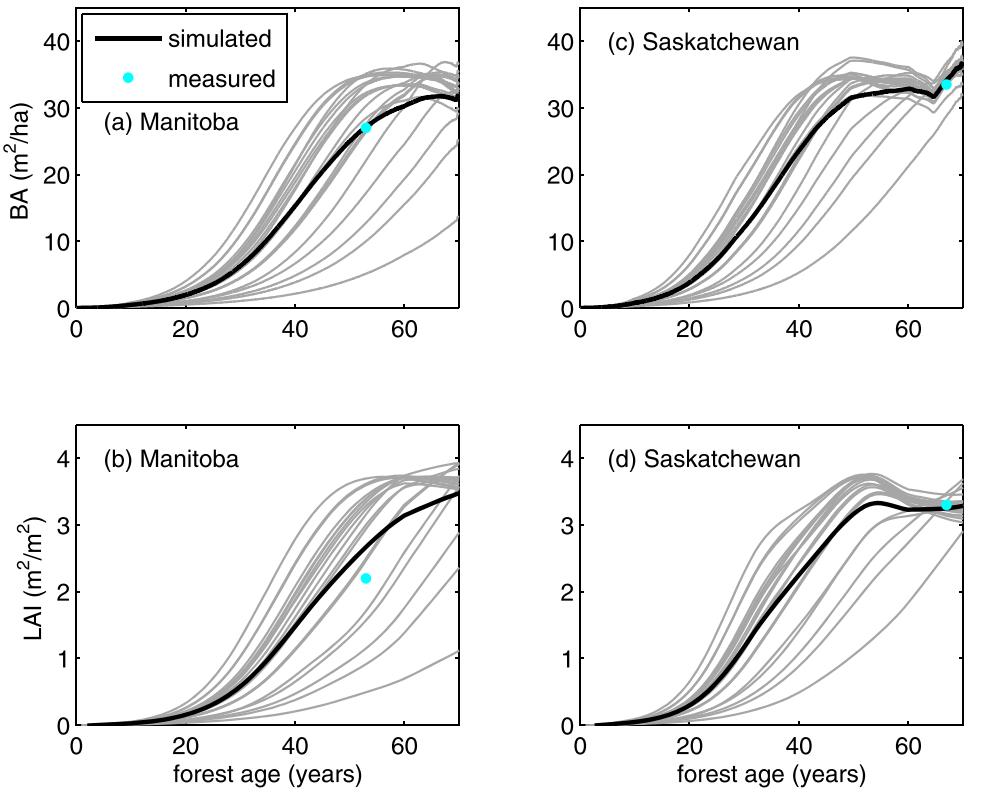

Figure 5. Comparison of simulated and observed aspen basal area (BA) and leaf are index (LAI) growth in central Canada. Simulated ensemble members (grey) and ensemble mean (black) of aspen forest growth are shown with measured forest chronosequence points (cyan). Measurements of LAI and BA were taken in the BOREAS Northern Study Area near Thompson, Manitoba (a-b) and the BOREAS Southern Study Area near Prince Albert (c-d).

The high percent error in basal area growth was due to an underprediction of the initial forest growth rate (Figure 6c) such that the ensemble mean underestimated forest basal area in the first 100 years (Figure 6c). This could be due to uncertainty in the initial organic layer depth at the beginning of the chronosequence; an initial overestimation of the organic layer thickness in our simulation would have decreased the black spruce basal accumulation rate in the first 100 years. However, around year 90, the simulated ensemble mean fell within the observed basal area range and after year 100, the ensemble mean and the majority of ensemble members fell within the observational range (Figure 6c). All ensemble members fell within the upper and lower decile bounds of observed organic layer depths in the moderately burned Quebec chronosequence (Figure 6d).

The overall range of uncertainty depicted by the different ensemble members was large in all of the forest chronosequences. For example, in the moderately burned Quebec chronosequence, individual ensemble members ranged from 6.0 to 45.4 m^2 ha^{-1} in basal area after 365 years. A similarly large spread was observed in many of the other basal area and LAI chronosequence validations (Table 6) despite the good agreement between the ensemble mean and the observations. Interestingly, the percent range in simulated organic layer depth chronosequences was much smaller than the percent range in aboveground forest growth metrics (Table 6). The large range in basal area and LAI of individual ensemble members was due mainly to model sensitivity to the range of measured values for V_{cmax} for both aspen and black spruce. The black spruce chronosequence in Manitoba was an exception; the maximum basal area and LAI were controlled mainly by the efficiency of nitrogen leaching. Uncertainty in the maximum seedling mortality rate of black spruce trees had little effect in the central Canada chronosequence validations. However, in the longer chronosequence validations in Quebec, the maximum seedling mortality exerted control over the slope of the decline in basal area in older black spruce forests (Figure 6c).

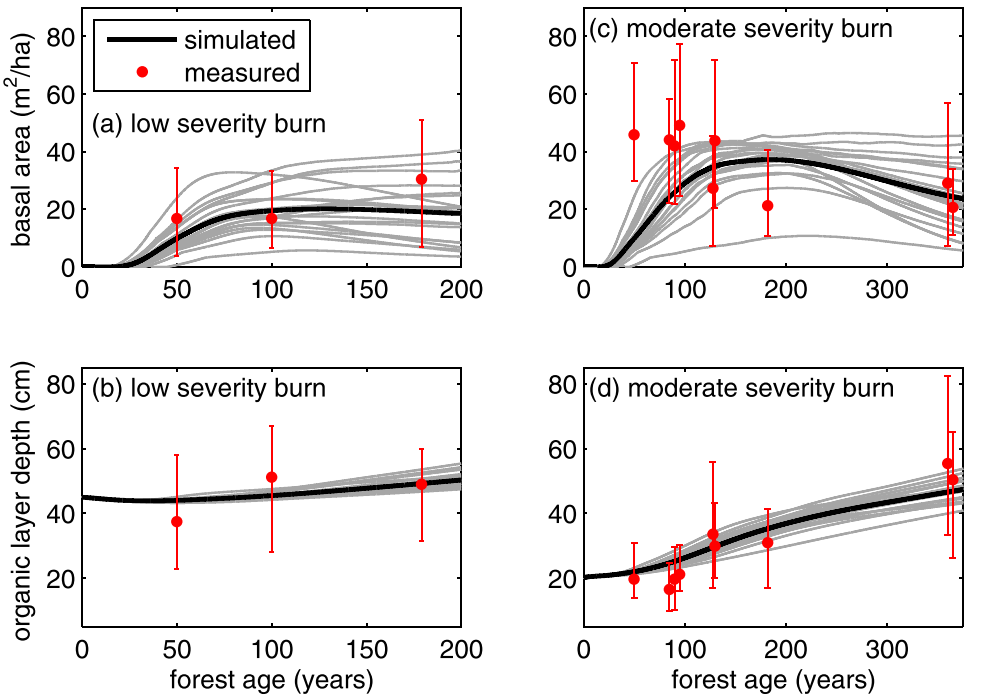

Figure 6. Comparison of simulated and observed black spruce basal area growth and organic layer accumulation in eastern Canada. Simulated ensemble members (grey) and ensemble mean (black) of black spruce forest basal area growth and organic layer accumulation are shown with measured forest chronosequence points (red). Error bars indicate the upper and lower decile bounds of the observations. Measurements of basal area (a,b) and organic layer depth (c,d) were made for a chronosequence occurring after a moderate fire (a,c) and a mild fire (b,d) in the Clay Belt region of Quebec.

3.2. Model Experiments

3.2.1. Forest Development After Fire Disturbance: Interactions Between Fire Severity, Forest Composition, and Ecosystem Carbon Storage

In our model, simulated postfire soil organic layer thickness controlled secondary succession after a fire disturbance event such that a thick organic layer prohibited aspen from establishing and increased black spruce seedling mortality. In thin organic layers, the time to succession between aspen and black spruce was controlled by the temperature regime and the availability of nutrients. In cooler regions such as Alaska, a shorter growing season and less productivity during the early and late growing season resulted in a maximum aspen biomass fraction of less than 0.5 and a shorter period of aspen presence (Figure 7a). In contrast, the longer growing season and increased precipitation in Manitoba and Quebec allowed for a longer duration of plant productivity and increased productivity during the early and late growing season. Increased growing season length and warmer summers favored aspen over black spruce growth, and resulted in a maximum aspen biomass fraction that was twice of that of Alaska (Figures 7b and 7c). However, because the total precipitation in Quebec was ~65% greater than in Manitoba, the simulated rate of nitrogen leaching was approximately 10 times greater in Quebec. This difference in nitrogen regimes shifted the competitive balance between aspen and black spruce, resulting in a shorter period of aspen dominance in Quebec relative to Manitoba (Figures 7b and 7c). When nitrogen leaching was excluded from the Quebec site, the period of aspen dominance became comparable to that of Manitoba.

Burn severity also had implications for total ecosystem carbon storage. Because simulations in the burn-severe experiment started out with very little residual soil organic layer, the difference in total ecosystem carbon between burn-severe (Figures 7d–7f) and burn-mild (Figures 7g–7i) was initially large. However, rapid secondary succession in the burn-severe simulation resulted in significant carbon accumulation during the first 350 years postdisturbance (Figures 7d–7f). In the burn-mild simulations (Figures 7g–7i), the initial ecosystem carbon was high due to a significant amount of soil carbon, but subsequent carbon accumulation was minimal or slightly negative due to low aboveground productivity and litter inputs into the soil organic layer. Despite the decreased aboveground productivity and litter inputs, some soil carbon lost

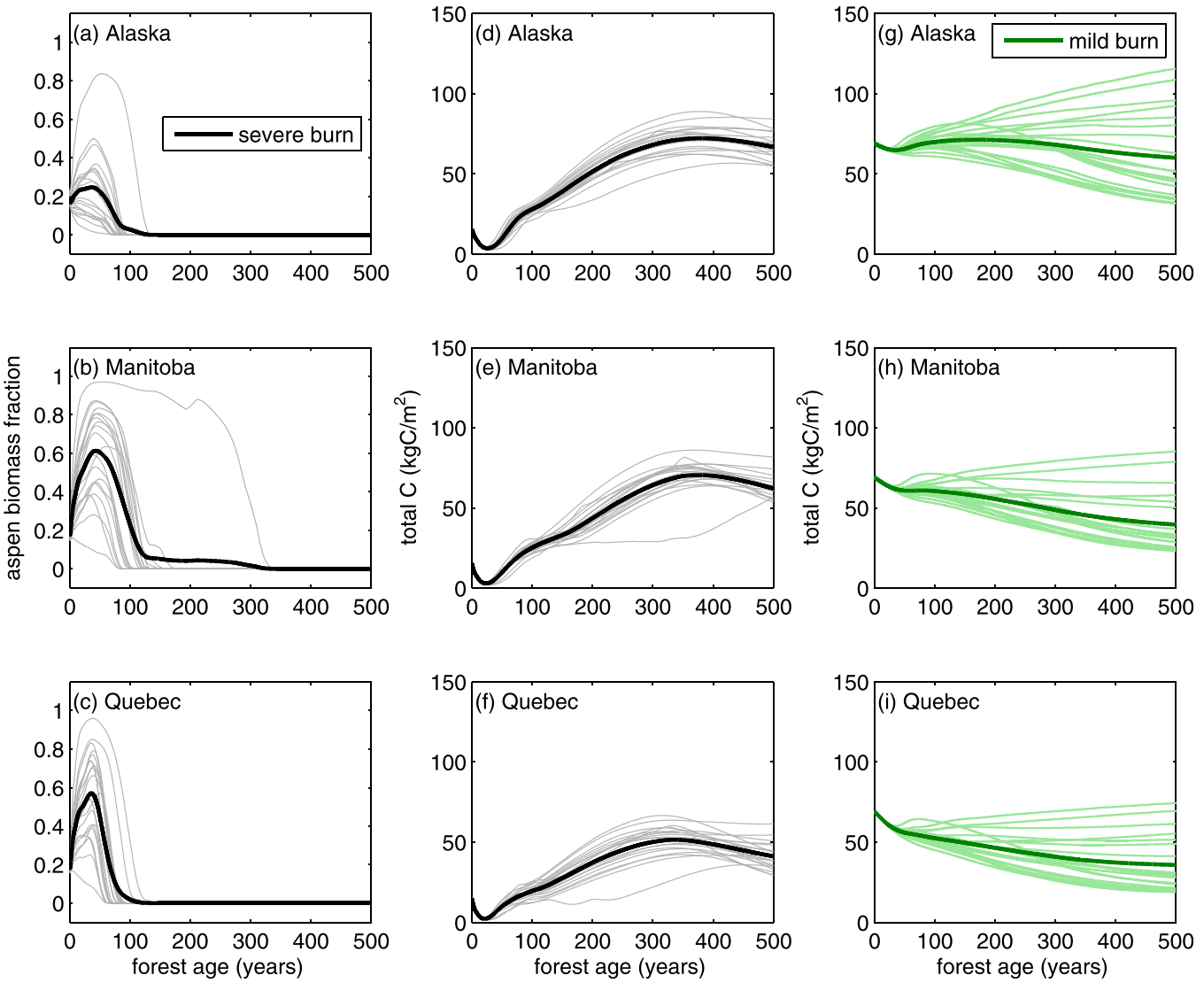

Figure 7. Simulated effects of fire severity on forest development. The left column (a-c) shows the ratio of aspen biomass to total plant biomass (aspen plus black spruce) in a forest recovering from a severe burn. The center column (d-f) shows total ecosystem carbon in a forest recovering from a severe burn. The right column (g-i) shows total ecosystem carbon in a forest recovering from a mild burn. The aspen biomass fraction in the case of the mild burn was zero for all locations. Individual ensemble members are shown with thin, light lines, and the ensemble mean is shown in thicker dark lines. All simulations were performed for locations near Delta Junction, Alaska (a,d,g), near Thompson, Manitoba (b,e,h), and near Abitibi, Quebec (c,f,i) for 500 years.

through decomposition was compensated for through moss growth. Independent of initial soil organic layer depth, older forests (> 350 years) converged into unproductive black spruce stands with roughly equivalent rates in organic layer accumulation constrained mainly by moss biomass accumulation (Figures 7d–7i). The range in the amount of carbon accumulated after 500 years between ensemble pairs was large in some cases. This variation was dependent mainly on model sensitivity to parameter values used for V_{cmax}.

3.2.2. Direct Effects of Soil Organic Layer on Forest Growth Ecosystem Carbon

We used six sets of simulations to disaggregate the biological and physical effects of the soil organic layer on forest structure and total ecosystem carbon in a forest developing after a mild burn. Because we expected that a thicker soil organic layer would affect forest outcome more strongly than a thinner soil organic layer, we adopt a mild burn disturbance scenario in this experiment. First, we ran one experiment using our standard parameterization that included both the dynamic organic layer and seedling mortality module (OLon-SMon). In this experiment, aspen trees were unable to grow owing to the thick soil organic layer (resulting in an aspen biomass fraction of zero) and slow ecosystem carbon accumulation owing to few litter inputs but steady moss accumulation (Figure 8). In our next experiment, we turned off the

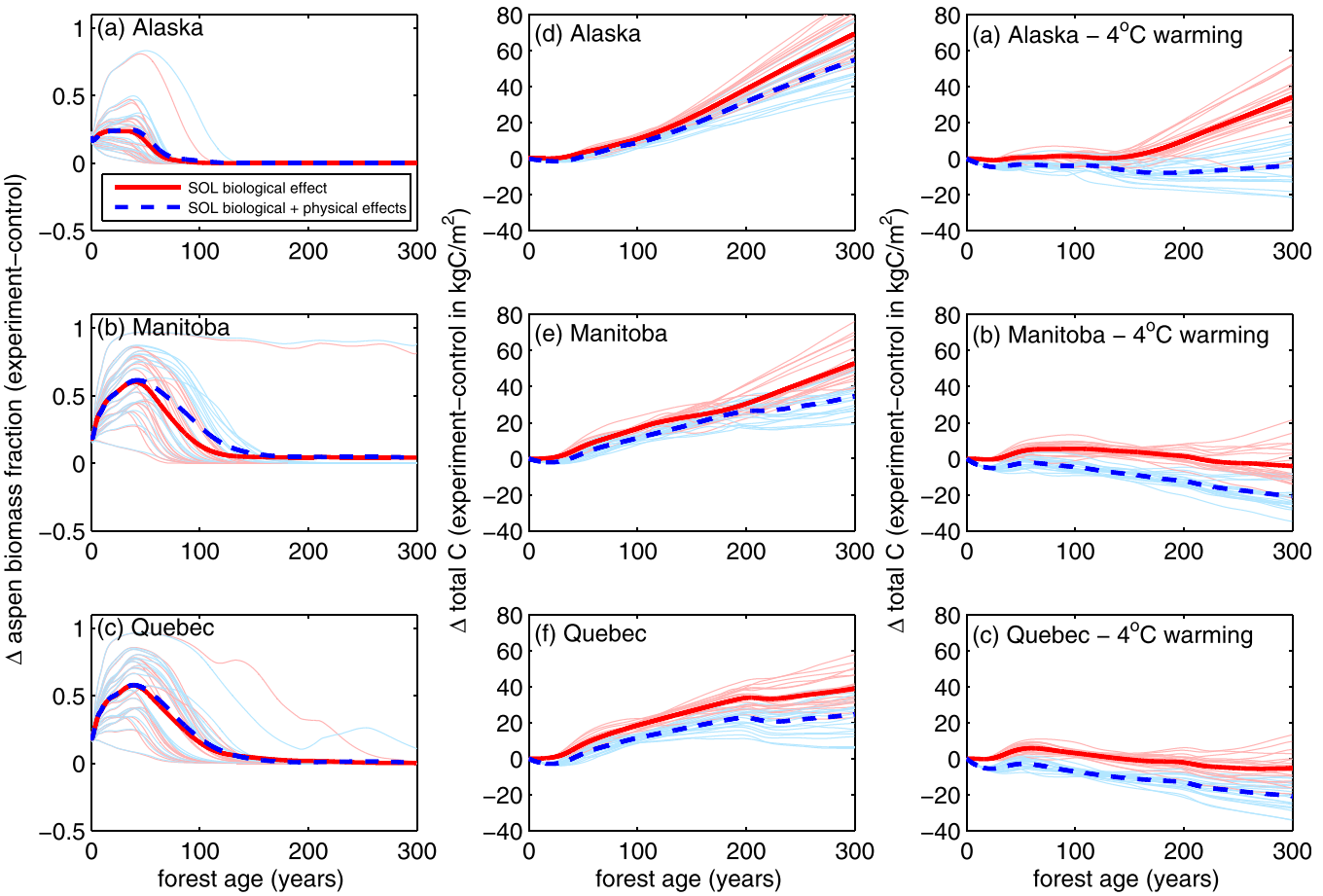

Figure 8. Simulated biological and physical effects of the soil organic layer on forest growth and ecosystem carbon storage. Here we simulated sets of ensembles to separate out the biological and physical effects of the soil organic layer on forest growth and ecosystem carbon storage in forests developing after a mild burn with an initial soil organic layer depth of 60 cm. We simulated one group of ensembles with a fully dynamic soil organic layer and organic layer-dependent seedling mortality (simulation OLon-SMon, Table 5), one without the biological effect of the soil organic layer where we turned off organic layer-dependent seedling mortality (OLon-SMoff), and one without both the physical and biological effect of the soil organic layer where we turned off dynamically accumulating soil organic layer and organic layer-dependent seedling mortality (OLoff-SMoff), further eliminating the impact of the soil organic layer on the soil thermal and moisture regimes. The left column (a-c) shows the change (either OLon-SMoff – Olon-SMon or OLoff-SMoff – Olon-SMon) in the ratio of aspen biomass to total plant biomass (aspen plus black spruce). The center column (d-f) shows the change in total ecosystem carbon. The right column (g-i) shows the change in total ecosystem carbon expected with a 4°C mean temperature increase. Individual ensemble members are shown with thin, light lines, and the ensemble mean is shown with a thicker, darker line. All simulations were performed for locations near Delta Junction, Alaska (a,d,g), near Thompson, Manitoba (b,e,h) and near Abitibi, Quebec (c,f,i) for a 300 year forest lifetime.

dependence of seedling mortality on organic layer depth to remove the biological effect of the soil organic layer (OLon-SMoff). In our third experiment, we turned off both dependence of seedling mortality on organic layer depth and the dynamic organic layer to remove both the biological and physical effects of the soil organic layer (OLoff-SMoff).

When comparing the ensemble mean difference between OLoff-SMoff and OLon-SMon, we found that neglecting the biological effect of the organic layer resulted in an overprediction of the presence of aspen in young forests in all locations (Figures 8a–8c) and in total ecosystem carbon throughout the simulation (Figures 8d–8f, blue line). This occurred because a higher rate of seedling survivorship (and subsequently more litter inputs) but a more rapid organic matter decomposition in OLoff-SMoff partially compensated for the lower seedling survivorship but slower decomposition and moss accumulation in OLon-SMon.

We illustrated these errors by disaggregating the biological and physical effects of the soil organic layer in OLon-SMoff, an experiment that did not include the biological effect of the organic layer but did include the physical effects of the soil organic layer on soil temperature, moisture, and organic matter decomposition. When we compared the ensemble mean difference between OLon-SMoff and OLon-SMon after 300 years, we found that total ecosystem carbon was a factor of two greater in OLon-SMoff compared to OLon-SMon at all locations (Figures 8d–8f). Total carbon accumulated much more rapidly in OLon-SMoff when

compared to OLoff-SMoff because the dynamically accumulating soil organic layer in OLon-SMoff included increased soil insulation, which significantly decreased the temperature at which decomposition occurred.

In our next three sets of simulations, we compounded the effect of a 4°C mean increase in temperature with our experiments examining the biological and physical effects of the soil organic layer. This set of experiments was designated as OLon-SMon-warm, OLon-SMoff-warm, and OLoff-SMoff-warm. Interestingly, compared to the suite of similar experiments without warming, we found a slightly negative ensemble mean difference in total ecosystem carbon storage between OLoff-SMoff-warm and OLon-SMon-warm in Quebec and Manitoba (Figures 8g–8i) due to the more rapid rate of soil organic matter decomposition in OLoff-SMoff-warm relative to OLon-SMon-warm. When compared to Figures 8d–8f, in Figures 8g–8i, we simulated a decreased biological effect of the soil organic layer because more rapid organic layer decomposition decreased the depth of the organic layer rapidly.

3.2.3. Effects of Projected Warming

In the T-2Cwarm and T-4Cwarm experiments, we found that an increase in the mean temperature changed forest composition in Alaska and Manitoba and ecosystem carbon accumulation at all locations. However, the magnitude and sign of the effect was location-specific and depended on the age of the forest. In Alaska and Manitoba, increased temperature increased the period of aspen dominance relative to T-0Cwarm (Figures 9a and 9b). This was due to two factors. First, increased temperature resulted in a longer growing season with increased productivity during the growing season (Figures 9g–9i). Second, warmer temperatures increased the rate of nitrogen cycling between T-0Cwarm and T-4Cwarm thereby increasing mineralized soil

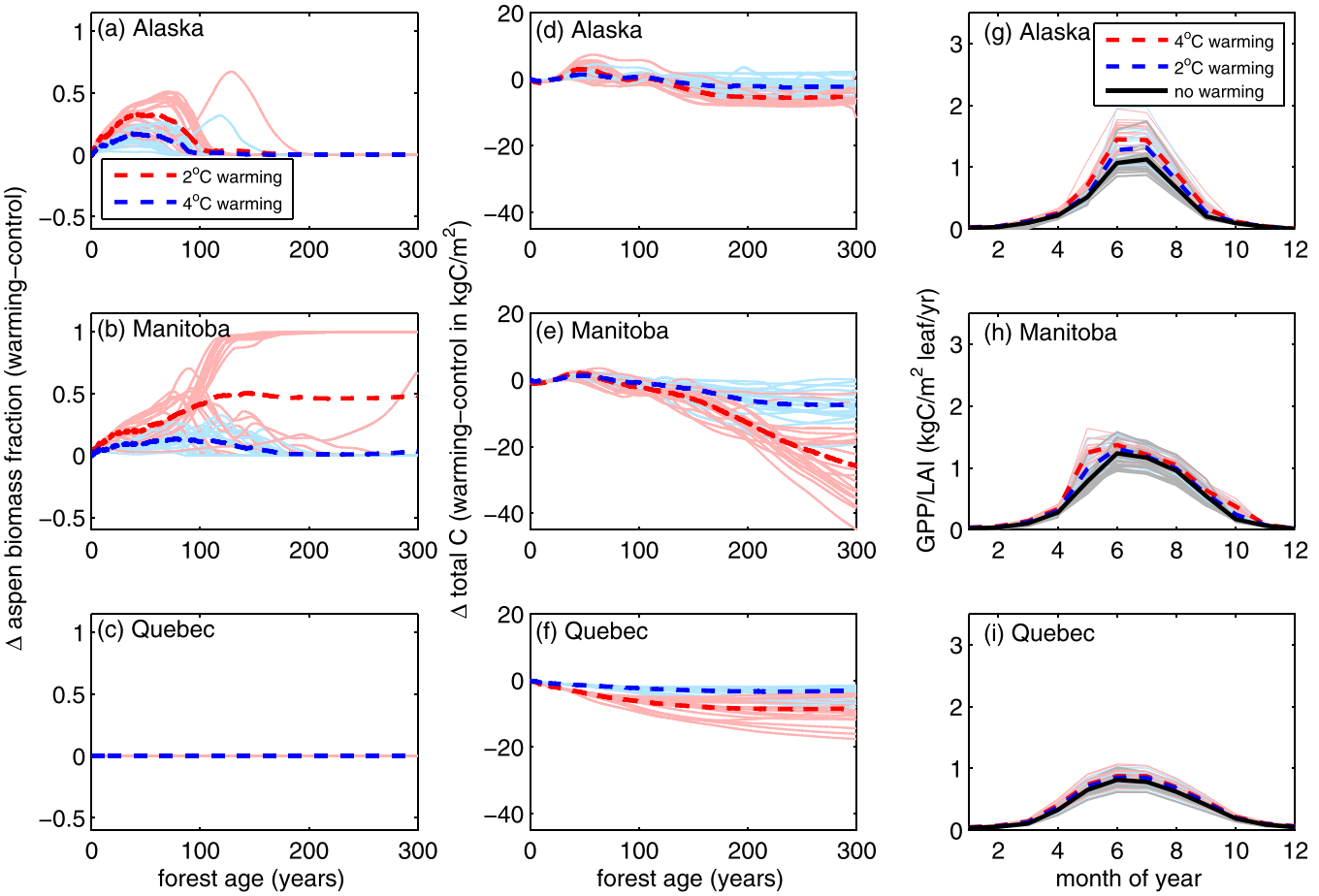

Figure 9. Simulated effects of projected increasing mean temperature on forest growth and ecosystem carbon storage for forests developing in the 21st century. Here we show the effects of a simulated 2°C mean warming (simulation T-2Cwarm, Table 5), and a 4°C mean warming (T-4Cwarm) relative to current temperatures (T-0Cwarm). The left column (a–c) shows change (either T-2Cwarm – T-0Cwarm or T-4Cwarm – T-0Cwarm) in ratio of aspen biomass to total plant biomass (aspen plus black spruce). The center column (d–f) shows change in total ecosystem carbon. The right column (g–i) shows ecosystem gross primary productivity (GPP) normalized by leaf area index (LAI) for an annual cycle. Individual ensemble members are shown with thin, light lines, and the ensemble mean is shown with a thicker, dark line. Simulations were performed for locations near Delta Junction, Alaska (a,d,g), near Thompson, Manitoba (b,e,h), and near Abitibi, Quebec (c,f,i) over a 300 year forest lifetime.

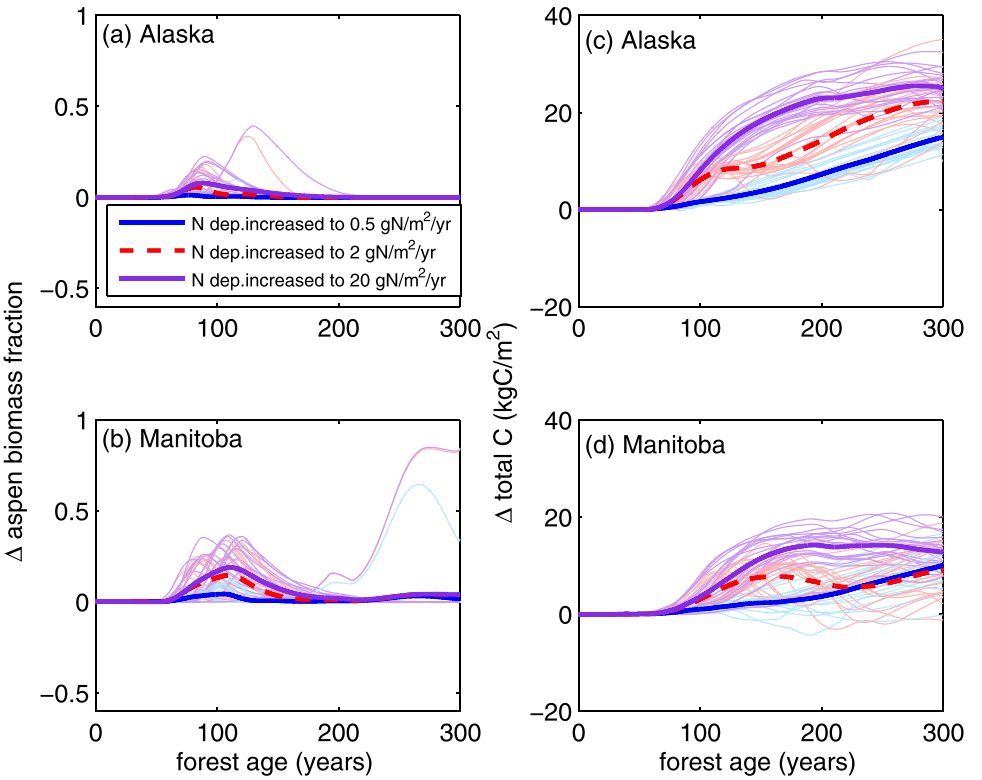

Figure 10. Simulated effects of changes in nitrogen deposition rates on forest growth and ecosystem carbon storage for forests developing in the 21st century. Here we show effects of increased nitrogen deposition rates on forest growth and carbon storage with nitrogen deposition scenarios of 2 g N m^{-2} yr^{-1} (simulation Ndep-2, Table 5) and 20 g N m^{-2} yr^{-1} (Ndep-20) relative to current deposition rates of 0.1 g N m^{-2} yr^{-1} (Ndep-0. 1) in Alaska and 0. 5 g N m^{-2} yr^{-1} (Ndep-0. 5) in Canada. The left column (a-b) shows the change (either Ndep-20 – Ndep-0.1, Ndep-2 – Ndep-0.1, or Ndep-0.5 – Ndep-0.1) in the ratio of aspen biomass to total plant biomass (aspen plus black spruce) and the right column (c-d) shows the change in total ecosystem carbon. Individual ensemble members are shown with thin, light lines, and the ensemble mean is shown with a thicker, darker line. All simulations were performed for locations near Delta Junction, Alaska (a,c), near Thompson, Manitoba (b-d), and near Abitibi, Quebec for a 300 year forest lifetime. However, plots for Quebec are not shown because there was no nitrogen limitation in the Quebec forest and thus no nitrogen fertilization effect.

nitrogen. As a result, aspen were able to grow and prevent black spruce seedlings from recruiting into the canopy for a longer period. In Alaska, the maximum aspen biomass fraction increased by ∼0.4 in the T-4Cwarm experiment relative to T-0Cwarm and the period of aspen dominance increased from 0 to ∼100 years (Figures 7a and 9a). However, because the growing season was still relatively short despite warming, black spruce recruitment was not fully inhibited and the forest eventually underwent succession to black spruce. In contrast, in the T-4Cwarm experiment in Manitoba, aspen productivity increased, particularly in the early spring (Figure 9h), to the point that it became difficult for black spruce to recruit seedlings and aspen produce multiple new cohorts. Depending on the value of V_{cmax} used for aspen and black spruce in a particular ensemble member, succession to black spruce might not have occurred or was delayed significantly (Figure 9b). Despite increased temperatures and nitrogen availability, a thick soil organic layer in Quebec prevented aspen from recruiting and black spruce perennially dominated (Figure 9c).

Simulated changes in forest composition with warming resulted in an initial (slight) increase in ecosystem carbon storage relative to T-0Cwarm in younger forests in Alaska and Manitoba due to increased aspen productivity (Figures 9d and 9e). No increase in storage was simulated in the spruce forests in Quebec (Figure 9f). After ∼100 years, there was a decrease in ecosystem carbon storage relative to T-0Cwarm at all locations due to slower soil carbon accumulation. The decrease in carbon storage in older forests was caused by increased temperature-dependent decomposition, and, to varying degrees, increased aspen litter inputs which decomposed more rapidly than black spruce litter and which also prevented moss carbon accumulation. These factors resulted in warmer soils (due to less insulation from a thinner soil organic layer) and faster organic matter decomposition. Particularly large losses in ecosystem carbon storage, on the order of 40%, were seen in Manitoba in T-4Cwarm due to the persistence of multiple cohorts of aspen (Figure 9e). In

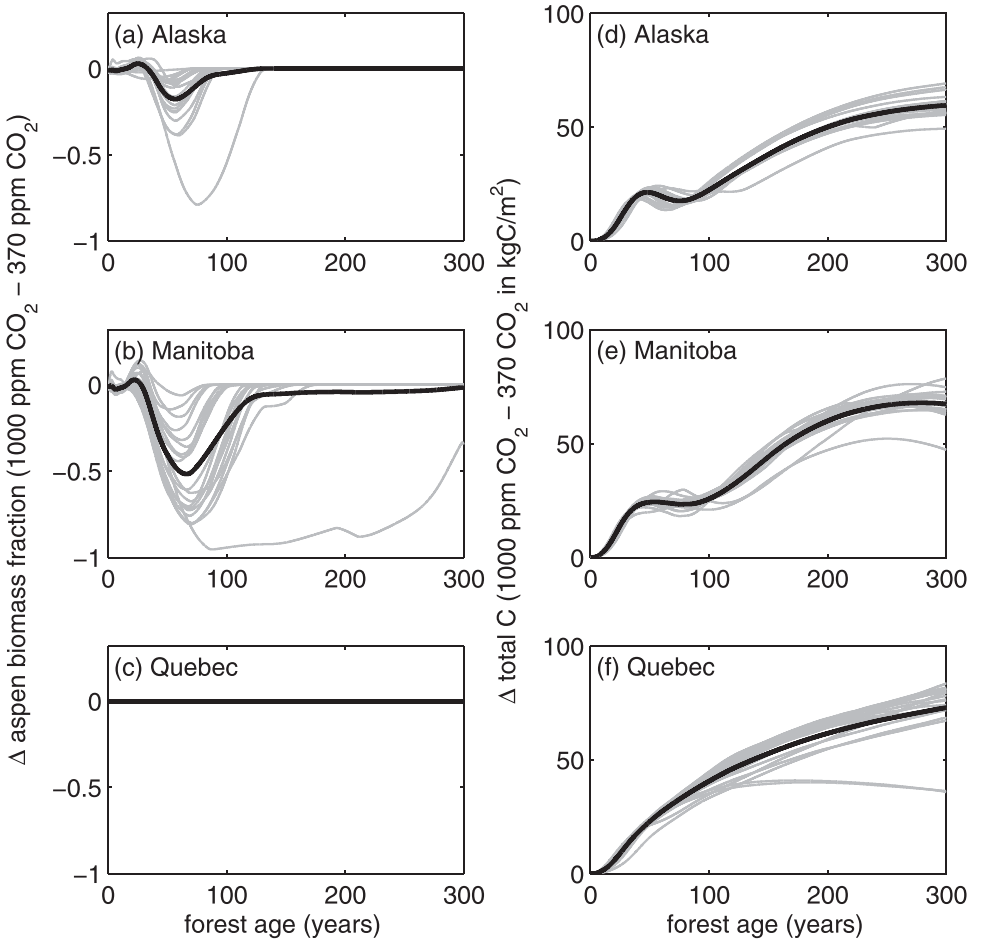

Figure 11. Simulated effects of increasing atmospheric CO_2 on forest growth and ecosystem carbon storage for forests developing in the 21st century. Here we show the effects of an increase in atmospheric CO_2 from 370 to 1000 ppm. The left column (a–c) shows change (simulations CO2-1000 − CO2-370, Table 5) in ratio of aspen biomass to total plant biomass (aspen plus black spruce). The right column (d-f) shows change in total ecosystem carbon. Individual ensemble members are shown with thin, light lines, and the ensemble mean is shown with a thicker, dark line. Simulations were performed for locations near Delta Junction, Alaska (a,d), near Thompson, Manitoba (b,e), and near Abitibi, Quebec (c,f) over a 300-year forest lifetime.

contrast, in Alaska and Quebec the simulated drop in ecosystem carbon between the T-0Cwarm and T-4Cwarm was <15% because black spruce was still able to recruit in the first century of forest growth.

3.2.4. Effects of Changing Nitrogen Deposition Rates

In our simulations, increased nitrogen deposition increased the period of aspen dominance in Manitoba (Figure 10b) and Alaska (Figure 10a). Interestingly, the effect of increasing nitrogen had a nonlinear effect on total ecosystem carbon accumulation in older forests depending on the location (Figures 10c, and 10d). In Alaska and Manitoba, increased nitrogen deposition increased the productivity and carbon accumulation in young forests. However, in Manitoba, increased persistence of multiple aspen cohorts due to increased nitrogen availability resulted in a decreased ability to accumulate carbon in older forests relative to Alaska. In Quebec, nitrogen deposition had no effect on forest growth or carbon accumulation because the forest was not nitrogen limited as a result of the thick soil organic layer, underlying clay mineral soil, and low nitrogen demand of black spruce trees.

3.2.4. Effects of Atmospheric CO_2 Fertilization

We found that an increase in atmospheric CO_2 from 370 to 1000 ppm changed forest composition in Alaska and Manitoba and increased ecosystem carbon accumulation at all locations. In Alaska and Manitoba, increased atmospheric CO_2 initially had a small positive effect on the aspen biomass fraction due to increased productivity from CO_2 fertilization (Figures 11a and 11b). This positive effect on aspen growth was followed by a stronger negative effect due to progressive nitrogen limitation (Figures 11a and 11b). No

aspen growth was simulated in Quebec as a result of the prohibitively thick soil organic layer (Figure 11c). At all locations, we simulated increased aboveground growth and litter inputs, which resulted in an increase in carbon accumulation by a factor of 2 or more after 300 years in experiment CO2-1000 relative to CO2-370 (Figures 11d–11f).

4. Discussion

The new model formulation presented here can inform Earth System Model (ESM) development in several ways. Most importantly, the species-specific effect of the soil organic layer on seedling recruitment and growth represents a critical step toward achieving an accurate North American boreal forest vegetation distribution as an emergent property of ESMs. We also find that the physical effects of the soil organic layer are important, and that our inclusion of a dynamic soil organic layer allows for a better simulation of the thermal and hydrological properties of the soil and the subsequent effects on decomposition and plant growth. Additionally, the new model formulation serves to improve the representation boreal of functional diversity in ESMs. Though it is not possible to include all individual NA boreal species in a global ESM, some species are sufficiently unique and important to warrant their own PFT. We argue that this is the case for black spruce, and maybe also for aspen because both are ecologically prevalent over a large geographic region in the NA boreal forest. Finally, our parameterization of moss growth, while empirical, highlights an important North American boreal ecosystem process that is neglected in many ESMs. Further implications and limitations of our analysis are discussed in the remainder of this section.

4.1. Uncertainty in Model Parameterizations

In this study, new modules related to soil organic matter accumulation and seedling mortality within ED2 were developed, parameterized, and tested against observations of NEP, inventory measurements of forest basal area, and chronosequences of forest basal area, LAI, soil organic layer depth, and soil carbon. As our simulation results show, incorporation of key feedbacks between soil organic layer thickness and aboveground forest growth [*Drobyshev et al*., 2010; *Johnstone and Chapin*, 2006a; *Johnstone et al*., 2010; *Lafleur et al*., 2010, 2015a; *Lecomte and Bergeron*, 2005] within our new NA boreal forest model enabled us to capture observed patterns of ecosystem dynamics on seasonal to multicentury timescales in different fire disturbance regimes.

Though the overall effect of the soil organic layer on seedling establishment is robustly observed, there is some debate in the literature about possible regional variations in the feedbacks between soil organic layer thickness and aboveground forest growth. *Greene et al*. [2007] and *Lafleur et al*. [2015a] each found a different organic layer depth interval over which aspen and black spruce seedling mortality increased when compared to the *Johnstone and Chapin* [2006a]. Additional measurements would be useful for model validations.

Moss has been shown to be an important component of the carbon balance in some boreal forests [*Goulden and Crill*, 1997]. However, it is not included in many boreal forest models [*Zhuang et al*., 2002]. Our model includes an empirical moss growth scheme based on a multicentury moss cover chronosequence. Our parameterization includes moss sensitivity to tree cover type (aspen versus black spruce); however, our model was parameterized using data only from one region in eastern Quebec and we do not explicitly treat the short timescale responses of moss growth to temperature and moisture regimes [*Williams and Flanagan*, 1996]. Therefore, our moss parameterization is not intended to represent interannual and shorter timescale variations in moss accumulation and should be further developed for other locations throughout the NA boreal forest. Moss physiological models are an active area of research [*Bona et al*., 2016; *Launiainen et al*., 2015], and we plan to include these dynamics into ED2-boreal in the future.

Chronosequences, which we employed as space-for-time substitution, were useful for evaluating the model's ability to simulate long-term forest growth. However, controlling for site-to-site variability in the chronosequences can be difficult [*Bond-Lamberty et al*., 2002b]. Immediate postfire forest conditions such as seedling density, soil nitrogen content, soil organic layer depth, and moss content were unknown. We handled this ambiguity by initializing all chronosequences for the same species-type (aspen or black spruce) with the same initial parameters, except in Quebec where data were available from which we could extrapolate the approximate initial soil organic layer depth. Given the uncertainty in the initial conditions of our

simulations, uncertainty in model parameters, and uncertainty in the observations themselves, it is expected that some discrepancies would exist between simulated and observed forest growth (Table 6).

We quantified the uncertainty associated with key model parameters by running ensembles composed of 20 members for each model validation and model experiment. These parameters included two parameters that the model is particularly sensitive to [*Dietze et al*., 2014] and two parameters that were important to our simulations but poorly constrained by experimental data. Each ensemble member featured a random draw from the joint prior probability density function defined from the literature or our own sensitivity tests (Table 2) for leaf biomass accumulation, V_{cmax}, maximum seedling mortality fraction, and nitrogen leaching efficiency. We found that tree growth was most affected by the variation in V_{cmax}. The spread among ensemble members was large when simulating long-term forest growth. Nevertheless, we found that the simulated ensemble mean did an overall realistic job of capturing forest basal area growth (Figures 4b,4c; 5a, 5c; 6a, 6c), LAI (Figures 4a; 5b, 5d), and soil organic layer accumulation (Figures 6b and 6d), as well as the age-related decline in LAI in older forests (Figures 4a; 5b, 5d). Based on the model's satisfactory performance against a diverse set of observations in multiple climate zones within the NA boreal forest, we argue that ED2-boreal is a useful tool in examining the ecosystem carbon budget in the NA boreal region.

4.2. Implications for Forest Composition

Over the next century, fire frequency, burn extent, and mean temperature are all projected to increase throughout the NA boreal forest [*Girardin et al*., 2013; *Hinzman et al*., 2013; *Kasischke and Turetsky*, 2006]. The increase in fire activity will likely correspond with a decrease in mean organic layer depth in most of the NA boreal forest [*Genet et al*., 2013; *Greene et al*., 2007], an increase in aspen seedling survivorship and a decrease in the mean forest age [*Kasischke and Turetsky*, 2006]. However, a decrease in the mean organic layer thickness is not likely to be uniform throughout the NA boreal forest due additional environmental factors. In the Clay Belt of Ontario and Quebec, all scenarios indicate that up to year 2100, low severity fires will be more common because paludification will likely be maintained under a warmer climate [*Lafleur et al*., 2015b]. This will generate more stands with thick soil organic layers that have a low probability of burning at high severity due to the waterlogging, poorly drained clay soils, and *Sphagnum* moss growth [*Terrier et al*., 2014].

In our simulations, increased mean temperature resulted in a longer growing season for deciduous forests with increased productivity during the growing season at all locations (Figures 9a–9c). However, trends in growing season productivity were not uniform throughout the climate gradient. In Manitoba, increased productivity was particularly noticeable in the early spring (May), but marginal when compared to the current temperature regime throughout the rest of the growing season (Figure 9h). In contrast, in Alaska, productivity increased significantly throughout the entire growing season with warming temperature (Figure 9g). Recent work quantifying possible effects of future climate scenarios on forest management strategies in eastern Canada similarly found a slight increase in aspen productivity, but a distinct decline in black spruce growth with warming [*Dhital et al*., 2015]. Our simulations showed only a marginal increase in black spruce productivity with warming in Quebec (Figure 9i), but this increase was significantly more pronounced in aspen forests in Alaska and Manitoba. In our simulations, younger forests with thinner postfire soil organic layers and longer/warmer growing seasons with more rapid nitrogen cycling were heavily populated with aspen. This indicates the possibility of a shift in forest composition toward increased aspen presence that can prevent black spruce recruitment. Such a regime shift has been suggested as a possible future trajectory based on both paleoforest analysis and changing climate conditions [*Bonan*, 2008; *Edwards et al*., 2005]. Interestingly, this shift to aspen dominance with changing climate seems to be more attributable to increasing temperature rather than CO_2 fertilization; we simulated that increasing CO_2 alone resulted in progressive nitrogen limitation [*Liu et al*., 2004] in aspen forests early on in during forest growth, ultimately resulting in a decline in aspen productivity (Figures 11a–11c). This possible shift to more broadleaf-dominated forest cover has implications not only for soil carbon storage, but could also feed back into the climate system through changes in energy partitioning between sensible and latent heat fluxes [*Hogg et al*., 2000] and changes in both summertime and wintertime surface albedo [*Liu et al*., 2005; *Lyons et al*., 2008], as well as reducing fire frequency and fire burn severity.

We also simulated significant diversity in regional responses to warmer temperatures, nitrogen limitation, and atmospheric CO_2. A mean warming of 4°C had the potential to decrease recruitment of black spruce

seedlings and shift forest composition so that multiple cohorts of aspen recruited in succession in Manitoba (Figure 9b). In Alaska, a shift to complete aspen dominance was not simulated in the 4°C warming scenario because the growing season remained sufficiently short and evergreen black spruce trees retained a competitive advantage against aspen trees. However, we did simulate an increased aspen presence in younger Alaskan forests (Figure 9a). With a fire return interval in Alaska of less than 100 years [*Kasischke and Turetsky*, 2006], a similar effect of persistent aspen presence could occur in Alaska, at least in the short term before the increased presence of aspen forest exerted a negative feedback on fire frequency. In Quebec, our simulations indicated that black spruce forests were less sensitive to changes in atmospheric CO_2, temperature, nitrogen, and fire activity than in western NA boreal forest. This difference was due to the robust presence of a thick soil organic layer projected to last throughout the 21st century [*Terrier et al*., 2014]. The presence of this thick soil organic layer allowed for black spruce recruitment in the absence of competition with aspen even with warmer conditions. Interestingly, our simulations also indicated that nitrogen limitation strongly regulated aspen forest growth [*Vadeboncoeur*, 2010]. This effect was particularly apparent in our atmospheric CO_2 fertilization experiments where increased aspen productivity due to higher atmospheric CO_2 was rapidly countered by progressive nitrogen limitation associated with the increased aspen nitrogen demand (Figures 11a and 11b).

4.3. Implications for Ecosystem Carbon Budgets

In our severe burn experiment, total ecosystem carbon accumulated rapidly after succession from aspen to black spruce and before the ecosystem became an unproductive old black spruce forest (Figures 7d–7f). These simulated middle-aged forests accumulated carbon at a rate of ~0.25 kg C m^{-2} yr^{-1}. Using ^{14}C dating, a previous study has reported water-logged black spruce stands accumulating 6–11 kg C m^{-2} over the period from ~1960 to 1995 (~0.17–0.31 kg C m^{-2} yr^{-1}) [*Trumbore and Harden*, 1997]. In upland black spruce stands, soil carbon has been observed to accumulate more slowly (~0.086 kg C m^{-2} yr^{-1}) but still at the same order of magnitude as our simulated accumulation rate [*Trumbore and Harden*, 1997]. These accumulation rates are remarkably large. If scaled to the area of the circumpolar boreal forest (1.2×10^7 km^2), the resulting rate would be about 3 Pg C yr^{-1} with further CO_2 fertilization over the 21st century potentially increasing this rate, depending on ecosystem response to changes in climate and nitrogen availability (Figures 11d–11f). This rate is comparable to the annual global carbon emissions resulting from the burning of fossil fuels (~9 Pg C yr^{-1}), underscoring the carbon mitigation potential of boreal forests.

However, our simulated ecosystem carbon accumulation should be interpreted as an upper bound for current boreal forest carbon accumulation potential for the following reasons. First, carbon accumulation rates slow with time since fire due to slower aboveground tree growth and fewer litter inputs (Figures 7d–7i), making it difficult to integrate values simulated or measured at an individual site to an entire region because of the heterogeneous spatial extent of forest age. Second, the NA boreal forest contains species other than black spruce and aspen, many of which accumulate significantly less soil carbon than black spruce stands [*Trumbore and Harden*, 1997]. Third, such an estimate does not include carbon released during forest disturbance events such as fire or insect attack which have the potential to change the behavior of the boreal forest from a carbon sink to a carbon source [*Kurz et al*., 2013]. Fourth, an implicit assumption of static environmental conditions is made. However, climate and disturbance event frequency and severity are both projected to change rapidly in the NA boreal forest and will affect the boreal forest carbon balance [*Kurz et al*., 2013]. Nevertheless, the impressive carbon storage capacity of middle-aged black spruce forests highlights the link between carbon management and forest management practices and emphasizes the need for proper forest management to preserve the NA boreal carbon sink with a changing fire cycle and warming temperatures in the 21st century.

With increasing temperature, we simulated a shift to more broadleaf-dominant forests where aspen were able to recruit multiple cohorts and prevent black spruce seedlings from recruiting. Such a change in NA boreal forest successional dynamics has the potential to decrease ecosystem carbon storage through increasing litter decay rates and decreasing moss accumulation [*Laganière et al*., 2010; *Légaré et al*., 2005]; the effect this shift would have on ecosystem carbon storage is dependent on the age of the forest. In warmer temperatures in younger forests (<100 years), we simulated that deciduous tree growth increased ecosystem carbon relative to black spruce growth due to increased aboveground productivity [*Cavard et al*., 2010]. In contrast, we simulated older forests that transition from black spruce-dominated to deciduous stands lost approximately 40% of their carbon storage potential (Figures 7e, 7f, 9e, and 9f). This reduction

occurred because aspen forests, as simulated, had less soil carbon accumulation due to more decomposable organic litter inputs, more rapid nitrogen cycling, and warmer soils that lacked insulating moss growth when compared to black spruce forests. However, recent work indicates that aspen forests tend to preserve more carbon than previously thought in deeper layers of the mineral soil due to fine root turnover and the relatively deep rooting system of aspen clones [*Laganière et al*., 2013]. In addition to potentially increasing the amount of soil carbon thought to be associated with aspen stands, soil carbon residing deep within the mineral soil layer would be more resistant to decomposition with warming temperatures. Nevertheless, an increase in aspen cover would have a major impact on the soil thermal regime [*Zhuang et al*., 2002], and could potentially increase soil temperatures in the top 20 cm by up to 7°C [*Jiang et al*., 2015]. Such a large temperature increase would significantly increase the rate of soil organic matter decomposition and carbon loss. In our experiments, we found that an increase in soil temperature associated with loss of the soil and moss organic layer resulted in a decrease of ∼15–20 kg C m^{-2} at all locations (Figures 8d–8f).

4.4. Comparison to Other Boreal Fire Disturbance Modeling Studies

Other terrestrial ecosystem modeling studies have previously recognized the necessity of integrating feedbacks between fire disturbance and the soil organic layer to capture soil thermal, hydrological, and biogeochemical dynamics in boreal forest ecosystems [*Carrasco et al*., 2006; *Yi et al*., 2010; *Zhuang et al*., 2002]. In work with a dynamic soil organic layer formulation of the Terrestrial Ecosystem Model (TEM), a new empirically parameterized moss layer and multiple soil carbon pools each with distinct porosity, bulk density, and decomposition rates are included [*Carrasco et al*., 2006; *Yi et al*., 2010; *Zhuang et al*., 2002]. With this implementation of TEM, *Carrasco et al*. [2006] and *Yi et al*. [2010] find that temperature and the soil thermal properties of the organic layer are important for preserving boreal forest soil carbon, citing a temperature gradient between surface and deep soils exceeding 10°C during the summer, which facilitates a 50–300% difference in midsummer decomposition between surface and deep soils of similar recalcitrance. *Bona et al*. [2016] further include six moss subpools divided into live, labile, and recalcitrant components for both feather and *Sphagnum* moss types with growth and decay rates empirically parameterized using various field sites throughout Canada. By including the moss submodel, *Bona et al*. [2016] find significant improvements in model-predicted soil carbon that are biased low by 40 Mg ha^{-1} when the moss submodel was not included. In ED2-boreal, we implement a comparable soil organic layer scheme, dividing the soil organic layer into an empirically parameterized moss layer and multiple soil carbon pools each with a different recalcitrance and bulk density. In our experiments, we similarly find that gradient in temperature between the surface and the base of soil organic layer can reach up to 15°C, doubling the temperature gradient between the surface and equivalent soil depth when compared to simulations with no insulating soil organic layer. Further, we find that the physical effect of the soil organic layer on the temperature of soil carbon decomposition results in approximately a 20–50% more carbon accumulation after 300 years when compared to simulations without the physical effect of the soil organic layer (Figures 8d–8f, difference between red and blue curves).

With this implementation of ED2-boreal, we found the biological effect of the soil organic layer on aboveground tree growth to also be important in projecting carbon storage capacity under warming temperatures because of the ability of the soil organic layer to mediate successional dynamics between early successional deciduous species and black spruce forests. *Yue et al*. [2013] similarly address boreal carbon dynamics after stand-replacing fire disturbances using the terrestrial biosphere model ORCHIDEE at multiple NA boreal forest sites. Despite the lack of some important features in their model such as the physical and biological effects of the soil organic layer and species types other than black spruce, *Yue et al*. [2013] were roughly able to postfire forest carbon dynamics when errors were upscaled across multiple sites. We build on the work by *Yue et al*. [2013] by further examining postfire successional dynamics between multiple forest species during different fire disturbance scenarios, and by capturing site-level carbon dynamics through our inclusion of interspecies competition and soil organic layer dynamics.

4.5. Limitations and Areas for Future Work

The primary purpose of this study was to examine the terrestrial carbon accumulation dynamics in the NA boreal forest. We did this for three different climate regimes within the NA boreal forests and looked at how changes with fire regime, temperature, nitrogen availability, and atmospheric CO_2 might affect ecosystem carbon storage potential. To isolate fire, temperature, nutrient, and CO_2 effects, we chose to use a simple

two-species system with only aspen and black spruce species-types. Though aspen and black spruce provide a reasonable and parsimonious representation of NA boreal forest species composition, they are not representative of the full species diversity present in the NA boreal forest which includes trees such as birch, jack pine, white spruce, balsam fir, tamarack, and alder, as well as various shrubs, graminoids, and mosses. Furthermore, our two-species set up does not allow for new species to migrate or replace aspen or black spruce as the dominant type of land cover. Rather, we are only able to examine the competitive dynamics between aspen and black spruce species-types with changes in environmental forcing. Additionally, some observations indicate that a number of boreal species are able to uptake organic nitrogen, alleviating some of the nitrogen stress due to a lack of available mineralized nitrogen [*Näsholm et al*., 1998; *Zhu and Zhuang*, 2013]. However, in the interest of parsimony, we did not include this process in our model. Finally, though we have extensively parameterized and tested our model with observations of near-surface soil organic layer processes in aspen and black spruce forests, our model has not been developed to capture dynamics of deep soil carbon formation and loss or the peat water-table feedback [*Ise et al*., 2008]. Accounting for some or all of these processes may be important when projecting changes in the carbon storage capacity in the NA boreal zone with warming temperatures, receding permafrost, and changing moisture regimes.

Some of our parameterizations, especially those related to moss, remain predominantly empirical. We see our empirical parameterizations of as an intermediate step between "no representation" and "full mechanistic representation" in models.

We are also working to improve the representations of functional diversity and fire in ED2-boreal. Though it will not be possible to include all individual NA boreal species in a global ESM, it has become apparent the increased functional diversity over current levels in global models is necessary to accurately capture forest carbon dynamics [*Fisher et al*., 2015; *Pavlick et al*., 2013]. We are currently carrying out modeling experiments of the NA boreal with increased numbers of plant functional types. We are also working on explicitly incorporating fire into our model. Multiple dynamic fire models with the necessary capabilities already exist [*Pfeiffer et al*., 2013], but it will be essential to evaluate model simulations of the interactions between fire severity, fire return interval, and long-term forest nitrogen dynamics [*Harden et al*., 2002].

5. Conclusions

We implemented new seedling survivorship and organic layer accumulation modules within an existing terrestrial biosphere model, allowing us to simulate the interdependence of seedling growth on soil organic layer thickness and the effects that the soil organic layer has on soil thermal and moisture regimes. By incorporating this interdependence, we were able to accurately simulate observed forest growth, ecosystem-level carbon fluxes, and soil organic layer dynamics after different fire disturbance scenarios along a climate gradient within the NA boreal forest.

Our study simulated surprisingly rapid carbon accumulation rates in middle-aged black spruce forests. These simulated rates were similar to previously measured carbon accumulation rates in water-logged black spruce stands, indicating the strong atmospheric CO_2 mitigation potential of the boreal black spruce forests and underscoring the need for proper forest management practices moving into the 21st century to preserve the NA boreal carbon sink with changing climate and fire regimes. In addition, our simulations linked a decrease in carbon accumulation with warming to a transition in forest cover that was $\sim$3 times greater than would be expected based on increased decomposition rates alone. Deciduous broadleaf forests, though initially more productive than evergreen needleleaf forests, did not promote surface organic layer accumulation in our model as a result of their decomposable litter inputs, lack of moss accumulation, and warm soils, which resulted in a significant decrease in carbon accumulation potential over the forest's lifetime. In contrast, evergreen needleleaf forests promoted significant surface organic layer accumulation in our model as a result of their slowly decomposing litter inputs, moss accumulation, and cool, moist soil conditions. This resulted in a $\sim$40% decrease in forest carbon accumulation over a 300-year forest lifetime in boreal forests that recruited multiple cohorts of broadleaf trees compared to boreal forests that underwent succession to needleleaf trees. Interestingly, nitrogen limitation potentially acted to increase boreal forest carbon accumulation by promoting succession from aspen forests (relatively poor in soil carbon) to black spruce forests (relatively rich in soil carbon) rather than allowing persistent aspen dominance with warmer temperatures.

Currently, global terrestrial biosphere models feature generic broadleaf and evergreen species-types in the NA boreal region and do not fully incorporate the observed dynamics between aboveground forest composition and soil carbon accumulation. Regional models do incorporate some of the important processes to varying degrees, but have generally been run at a much smaller scale than the NA boreal forest. The new model feedbacks reported here have the potential to significantly improve projections of future carbon storage in the NA boreal forest when compared to previous model schemes because of the important link between carbon accumulation and forest cover. Continued assessment of the impacts that climate change will have on aboveground forest composition and soil organic layer accumulation using species-types specific to the NA boreal zone remains an important task for our understanding of short and long-term behavior of the forest growth and terrestrial carbon dynamics in the boreal forest.

Acknowledgments

The authors gratefully acknowledge support from a National Science Foundation Graduate Research Fellowship to A.T.T. (DGE 1148900) and from the NASA Carbon Cycle Science Program Award NNX11AD45G to D.M. The authors thank the students in the Medvigy laboratory, Hélèn Genet, Jill Johnstone, David McGuire, Steve Pacala, Jorge Sarmiento, Justin Sheffield, and Aurélie Terrier and two anonymous reviewers for their insightful suggestions. The authors also thank Benjamin Bond-Lamberty for his assistance and generosity in providing data used to parameterize diagnostic relations between tree diameter at breast height and plant biomass. The authors declare no conflicts of interest. Data from the model simulations is freely and publicly available on the Princeton DataSpace Repository (http://arks.princeton.edu/ark:/88435/dsp01cf95jd86d). Model source code is available as a supporting information file.

References

Abidine, A. Z., P. Y. Bernier, and A. P. Plamondon (1994), Water relation parameters of lowland and upland black spruce: Seasonal variation and ecotypic differences, *Can. J. For. Res.*, *24*, 587–593.

Allen, M. R., and W. J. Ingram (2002), Constraints on future changes in climate and the hydrologic cycle, *Nature*, *419*, 224–232, doi:10.1038/nature01092.

Balducci, L., A. Deslauriers, A. Giovannelli, M. Beaulieu, S. Delzon, S. Rossi, and C. B. Rathgeber (2015), How do drought and warming influence survival and wood traits of Picea mariana saplings?, *J. Exp. Botany*, *66*(1), 377–389, doi:10.1093/jxb/eru431.

Bergeron, Y., and N. J. Fenton (2012), Boreal forests of eastern Canada revisited: Old growth, nonfire disturbances, forest succession, and biodiversity, *Botany*, *90*(6), 509–523, doi:10.1139/b2012-034.

Bergeron, Y., M. D. Flannigan, S. Gauthier, A. Leduc, and P. Lefort (2004), Past, current and future fire frequency in the canadian boreal forest: Implications for sustainable forest management, *AMBIO*, *33*(6), 356–360, doi:10.1579/0044-7447-33.6.356.

Bona, K. A., C. H. Shaw, J. W. Fyles, and W. A. Kurz (2016), Modelling moss-derived carbon in upland black spruce forests, *Can. J. For. Res.*, *46*, 520–534, doi:10.1139/cjfr-2015-0512.

Bonan, G. B. (2008), Forests and climate change: Forcings, feedbacks, and the climate benefits of forests, *Science*, *320*(5882), 1444–1449, doi:10.1126/science.1155121.

Bond-Lamberty, B., C. Wang, and S. T. Gower (2002a), Aboveground and belowground biomass and sapwood area allometric equations for six boreal tree species of northern Manitoba, *Can. J. For. Res.*, *32*(8), 1441–1450, doi:10.1139/x02-063.

Bond-Lamberty, B., C. Wang, S. T. Gower, and J. Norman (2002b), Leaf area dynamics of a boreal black spruce fire chronosequence, *Tree Physiol.*, *22*(14), 993–1001.

Bond-Lamberty, B., S. T. Gower, C. Wang, P. Cyr, and H. Veldhuis (2006), Nitrogen dynamics of a boreal black spruce wildfire chronosequence, *Biogeochemistry*, *81*(1), 1–16, doi:10.1007/s10533-006-9025-7.

Bond-Lamberty, B., A. V. Rocha, K. Calvin, B. Holmes, C. Wang, and M. L. Goulden (2014), Disturbance legacies and climate jointly drive tree growth and mortality in an intensively studied boreal forest, *Global Change Biol.*, *20*(1), 216–227, doi:10.1111/gcb.12404.

Carrasco, J. J., J. C. Neff, and J. W. Harden (2006), Modeling physical and biogeochemical controls over carbon accumulation in a boreal forest soil, *J. Geophys. Res.*, *111*, G02004, doi:10.1029/2005JG000087.

Cavard, X., Y. Bergeron, H. Y. H. Chen, and D. Paré (2010), Mixed-species effect on tree aboveground carbon pools in the east-central boreal forests, *Can. J. For. Res.*, *40*(1), 37–47, doi:10.1139/x09-171.

de Groot, W. J., P. M. Bothwell, D. H. Carlsson, and K. A. Logan (2003), Simulating the effects of future fire regimes on western Canadian boreal forests, *J. Veget. Sci.*, *14*, 355–264.

Dhital, N., F. Raulier, P. Y. Bernier, M.-P. Lapointe-Garant, F. Berninger, and Y. Bergeron (2015), Adaptation potential of ecosystem-based management to climate change in the eastern Canadian boreal forest, *J. Environ. Plann. Manage.*, *58*(12), 1–22, doi:10.1080/09640568.2014.978079.

Dietze, M. C., et al. (2014), A quantitative assessment of a terrestrial biosphere model's data needs across North American biomes, *J. Geophys. Res. Biogeosci.*, *119*, 286–300, doi:10.1002/2013JG002392.

Drobyshev, I., M. Simard, Y. Bergeron, and A. Hofgaard (2010), Does soil organic layer thickness affect climate–growth relationships in the black spruce boreal ecosystem?, *Ecosystems*, *13*(4), 556–574, doi:10.1007/s10021-010-9340-7.

Drobyshev, I., S. Gewehr, F. Berninger, Y. Bergeron, and M. McGlone (2013), Species specific growth responses of black spruce and trembling aspen may enhance resilience of boreal forest to climate change, *J. Ecol.*, *101*(1), 231–242, doi:10.1111/1365-2745.12007.

Edwards, M. E., L. B. Brubaker, A. V. Lozhkin, and P. M. Anderson (2005), Structurally novel biomes: A response to past warming in Beringia, *Ecology*, *86*(7), 1696–1703.

Euskirchen, E. S., A. D. McGuire, F. S. Chapin, III, S. Yi, and C. C. Thompson (2009), Changes in vegetation in northern Alaska under scenarios of climate change, 2003-2100: Implications for climate feedbacks, *Ecol. Appl.*, *19*(4), 1022–1043, doi:10.1890/08-0806.1.

Euskirchen, E. S., T. B. Carman, and A. D. McGuire (2014), Changes in the structure and function of northern Alaskan ecosystems when considering variable leaf-out times across groupings of species in a dynamic vegetation model, *Global Change Biol.*, *20*(3), 963–978, doi:10.1111/gcb.12392.

Fenton, N. J., and Y. Bergeron (2006), Facilitative succession in a boreal bryophyte community driven by changes in available moisture and light, *J. Veg. Sci.*, *17*(1), 65–76, doi:10.1111/j.1654-1103.2006.tb02424.x.

Fenton, N. J., N. Lecomte, S. Légaré, and Y. Bergeron (2005), Paludification in black spruce (Picea mariana) forests of eastern Canada: Potential factors and management implications, *For. Ecol. Manage.*, *213*(1–3), 151–159, doi:10.1016/j.foreco.2005.03.017.

Fenton, N. J., S. Légaré, Y. Bergeron, and D. Paré (2006), Soil oxygen within boreal forests across an age gradient, *Can. J. Soil Sci.*, *86*, 1–9.

Fisher, R. A., et al. (2015), Taking off the training wheels: The properties of a dynamic vegetation model without climate envelopes, CLM4.5(ED), *Geosci. Model Dev.*, *8*(11), 3593–3619, doi:10.5194/gmd-8-3593-2015.

Genet, H., et al. (2013), Modeling the effects of fire severity and climate warming on active layer thickness and soil carbon storage of black spruce forests across the landscape in interior Alaska, *Environ. Res. Lett.*, *8*(4), 045016, doi:10.1088/1748-9326/8/4/045016.

Gerber, S., and E. J. Brookshire (2014), Scaling of physical constraints at the root-soil interface to macroscopic patterns of nutrient retention in ecosystems, *Am. Nat.*, *183*(3), 418–430.
Girardin, M. P., A. A. Ali, C. Carcaillet, S. Gauthier, C. Hély, H. Le Goff, A. Terrier, and Y. Bergeron (2013), Fire in managed forests of eastern Canada: Risks and options, *For. Ecol. Manage.*, *294*, 238–249, doi:10.1016/j.foreco.2012.07.005.
Girardin, M. P., X. J. Guo, R. De Jong, C. Kinnard, P. Bernier, and F. Raulier (2014), Unusual forest growth decline in boreal North America covaries with the retreat of Arctic sea ice, *Global Change Biol.*, *20*(3), 851–866, doi:10.1111/gcb.12400.
Goulden, M. L., and P. M. Crill (1997), Automated measurements of CO2 exchange at the moss surface of a black spruce forest, *Tree Physiol.*, *17*, 537–542.
Greene, D. F., J. Noël, Y. Bergeron, M. Rousseau, and S. Gauthier (2004), Recruitment ofPicea mariana,Pinus banksiana, andPopulus tremuloidesacross a burn severity gradient following wildfire in the southern boreal forest of Quebec, *Can. J. For. Res.*, *34*(9), 1845–1857, doi:10.1139/x04-059.
Greene, D. F., et al. (2007), The reduction of organic-layer depth by wildfire in the North American boreal forest and its effect on tree recruitment by seed, *Can. J. For. Res.*, *37*(6), 1012–1023, doi:10.1139/x06-245.
Harden, J. W., M. Mack, H. Veldhuis, and S. T. Gower (2002), Fire dynamics and implications for nitrogen cycling in boreal forests, *J. Geophys. Res.*, *108*(D3), 8223, doi:10.1029/2001JD000494.
Harden, J. W., K. L. Manies, J. O'Donnell, K. Johnson, S. Frolking, and Z. Fan (2012), Spatiotemporal analysis of black spruce forest soils and implications for the fate of C, *J. Geophys. Res.*, *117*, G01012, doi:10.1029/2011JG001826.
Hinzman, L. D., C. J. Deal, A. D. McGuire, S. H. Mernild, I. V. Polyakov, and J. E. Walsh (2013), Trajectory of the Arctic as an integrated system, *Ecol. Appl.*, *23*(8).
Hogg, E. H., D. T. Price, and T. A. Black (2000), Postulated feedbacks of deciduous forest phenology on seasonal climate patterns in the western Canadian interior, *J. Clim.*, *13*(24), 4229–4243, doi:10.1175/1520-0442(2000)013 < 4229:PFODFP>2.0.CO;2.
Hom, J., and W. C. Oechel (1983), The photosynthetic capacity, nutrient content, and nutrient use efficiency of different needle age-classes of black spruce (*Picea mariana*) found in interior Alaska, *Can. J. For. Res.*, *13*, 834–839.
Intergovernmental Panel on Climate Change (IPCC) (2013) IPCC Fifth Assessment Report: Climate Change 2013 (AR5), Cambridge University Press, Geneva, Switzerland.
Ise, T., A. L. Dunn, S. C. Wofsy, and P. R. Moorcroft (2008), High sensitivity of peat decomposition to climate change through water-table feedback, *Nat. Geosci.*, *1*(11), 763–766, doi:10.1038/ngeo331.
Jeong, S.-J., and D. Medvigy (2014), Macroscale prediction of autumn leaf coloration throughout the continental United States, *Global Ecol. Biogeogr.*, *23*(11), 1245–1254, doi:10.1111/geb.12206.
Jerabkova, L., C. E. Prescott, and B. E. Kishchuk (2006), Nitrogen availability in soil and forest floor of contrasting types of boreal mixedwood forests, *Can. J. For. Res.*, *36*(1), 112–122, doi:10.1139/x05-220.
Jiang, Y., A. V. Rocha, J. A. O'Donnell, J. A. Drysdale, E. B. Rastetter, G. R. Shaver, and Q. Zhuang (2015), Contrasting soil thermal responses to fire in Alaskan tundra and boreal forest, *J. Geophys. Res. Earth Surf.*, *120*, 363–378, doi:10.1002/2014JF003180.
Johnstone, J. F., and F. S. Chapin (2006a), Effects of soil burn severity on post-fire tree recruitment in Boreal forest, *Ecosystems*, *9*(1), 14–31, doi:10.1007/s10021-004-0042-x.
Johnstone, J. F., and F. S. Chapin (2006b), Fire interval effects on successional trajectory in Boreal Forests of Northwest Canada, *Ecosystems*, *9*(2), 268–277, doi:10.1007/s10021-005-0061-2.
Johnstone, J. F., T. N. Hollingsworth, F. S. Chapin, and M. C. Mack (2010), Changes in fire regime break the legacy lock on successional trajectories in Alaskan boreal forest, *Global Change Biol.*, *16*(4), 1281–1295, doi:10.1111/j.1365-2486.2009.02051.x.
Kasischke, E. S., and M. R. Turetsky (2006), Recent changes in the fire regime across the North American boreal region: Spatial and temporal patterns of burning across Canada and Alaska, *Geophys. Res. Lett.*, *33*, L09703, doi:10.1029/2006GL025677.
Kubiske, M. E., K. S. Pregitzer, C. J. Mikan, D. R. Zak, J. L. Maziasz, and A. Teeri (1997), Populus tremuloides photosynthesis and crown architecture in response to elevated CO2 and soil N availability, *Oecologia*, *110*(3), 328–336.
Kurz, W. A., C. H. Shaw, C. Boisvenue, G. Stinson, J. Metsaranta, D. Leckie, A. Dyk, C. Smyth, and E. T. Neilson (2013), Carbon in Canada's boreal forest: A synthesis1, *Environ. Rev.*, *21*(4), 260–292, doi:10.1139/er-2013-0041.
La Roi, G. H., and M. H. L. Stringer (1976), Ecological studies in the boreal spruce-fir forests of the North American taiga. II. Analysis of the bryophyte flora, *Can. J. Botany*, *54*, 619–643.
Lafleur, B., N. J. Fenton, D. Paré, M. Simard, and Y. Bergeron (2010), Contrasting Effects of Season and Method of Harvest on Soil Properties and the Growth of Black Spruce Regeneration in the Boreal Forested Peatlands of Eastern Canada, *Silva Fennica*, *44*(5), 799–813.
Lafleur, B., A. Cazal, A. Leduc, and Y. Bergeron (2015a), Soil organic layer thickness influences the establishment and growth of trembling aspen (Populus tremuloides) in boreal forests, *For. Ecol. Manage.*, *347*, 209–216.
Lafleur, B., N. J. Fenton, and Y. Bergeron (2015b), Forecasting the development of boreal paludified forests in response to climate change: A case study using Ontario ecosite classification, *For. Ecosyst.*, *2*(1), 1–11, doi:10.1186/s40663-015-0027-6.
Laganière, J., D. Paré, and R. L. Bradley (2010), How does a tree species influence litter decomposition? Separating the relative contribution of litter quality, litter mixing, and forest floor conditions, *Can. J. For. Res.*, *40*(3), 465–475, doi:10.1139/x09-208.
Laganière, J., D. A. Angers, D. Paré, Y. Bergeron, and H. Y. H. Chen (2011), Black spruce soils accumulate more uncomplexed organic matter than Aspen soils, *Soil Sci. Soc. Am. J.*, *75*(3), 1125–1132, doi:10.2136/sssaj2010.0275.
Laganière, J., D. Paré, Y. Bergeron, H. Y. H. Chen, B. W. Brassard, and X. Cavard (2013), Stability of soil carbon stocks varies with forest composition in the Canadian Boreal Biome, *Ecosystems*, *16*(5), 852–865, doi:10.1007/s10021-013-9658-z.
Launiainen, S., G. G. Katul, A. Lauren, and P. Kolari (2015), Coupling boreal forest CO2, H2O and energy flows by a vertically structured forest canopy: Soil model with separate bryophyte layer, *Ecol. Modell.*, *312*, 385–405, doi:10.1016/j.ecolmodel.2015.06.007.
Lavoie, M., D. Paré, and Y. Bergeron (2005), Impact of global change and forest management on carbon sequestration in northern forested peatlands, *Environ. Rev.*, *13*(4), 199–240, doi:10.1139/a05-014.
Lecomte, N., and Y. Bergeron (2005), Successional pathways on different surficial deposits in the coniferous boreal forest of the Quebec Clay Belt, *Can. J. For. Res.*, *35*(8), 1984–1995, doi:10.1139/x05-114.
Légaré, S., D. Paré, and Y. Bergeron (2005), Influence of Aspen on forest floor properties in black spruce-dominated stands, *Plant Soil*, *275*(1–2), 207–220, doi:10.1007/s11104-005-1482-6.
Liu, H. P., J. T. Randerson, J. Lindfors, and F. S. Chapin III (2005), Changes in the surface energy budget after fire in boreal ecosystems of interior Alaska: An annual perspective, *J. Geophys. Res.*, *110*, D13101, doi:10.1029/2004JD005158.
Liu, Y., et al. (2004), Progressive nitrogen limitation of ecosystem responses to rising atmospheric carbon dioxide, *BioScience*, *54*(8), 731–739, doi: 10.1641/0006-3568(2004)054[0731:PNLOER]2.0.CO;2

Lyons, E. A., Y. Jin, and J. T. Randerson (2008), Changes in surface albedo after fire in boreal forest ecosystems of interior Alaska assessed using MODIS satellite observations, *J. Geophys. Res.*, *113*, G02012, doi:10.1029/2007JG000606.
Malone, T., J. Liang, and E. C. Packee (2009), Cooperative Alaska Forest Inventory, *Gen. Tech. Re. PNW-GTR-785*, 42 p., U.S. Dep. Agric. For. Serv. Pac. Northwest Res. Stn., Portland, Oreg.
McCumber, M. C., and R. A. Pielke (1981), Simulation of the effects of surface fluxes of heat and moisture in a mesoscale numerical model: 1. Soil layer, *J. Geophys. Res.*, *86*(C10), 9929–9938, doi:10.1029/JC086iC10p09929.
Medvigy, D., and P. R. Moorcroft (2012), Predicting ecosystem dynamics at regional scales: An evaluation of a terrestrial biosphere model for the forests of northeastern North America, *Philos. Trans. R. Soc. London Ser. B*, *367*(1586), 222–235, doi:10.1098/rstb.2011.0253.
Medvigy, D., S. C. Wofsy, J. W. Munger, D. Y. Hollinger, and P. R. Moorcroft (2009), Mechanistic scaling of ecosystem function and dynamics in space and time: Ecosystem Demography model version 2, *J. Geophys. Res.*, *114*, G01002, doi:10.1029/2008JG000812.
Moorcroft, P. R., G. C. Hurtt, and S. W. Pacala (2001), A method for scaling vegetation dynamics: The ecosystem demography model (ED), *Ecol. Monogr.*, *71*(4), 557–585, doi: 10.1890/0012-9615(2001)071[0557:AMFSVD]2.0.CO;2.
Näsholm, T., A. Ekblad, A. Nordin, R. Giesler, M. Högberg, and P. Högberg (1998), Boreal forest plants take up organic nitrogen, *Nature*, *392*, 914–916.
Natalia, S., V. J. Lieffers, and S. M. Landhäusser (2008), Effects of leaf litter on the growth of boreal feather mosses: Implication for forest floor development, *J. Veg. Sci.*, *19*(2), 253–260, doi:10.3170/2008-8-18367.
Nowak, R. S., D. S. Ellsworth, and S. D. Smith (2004), Functional responses of plants to elevated atmospheric CO2- do photosynthetic and productivity data from FACE experiments support early predictions?, *New Phytol.*, *162*(2), 253–280, doi:10.1111/j.1469-8137.2004.01033.x.
Oleson, K. W., D. M. Lawrence, G. B. Gordon, M. G. Flanner, E. Kluzek, J. P. Lawrence, S. Levis, S. C. Swenson, P. E. Thorton (2010), Technical description of version 4.0 of the Community Land Model (CLM).
Pavlick, R., D. T. Drewry, K. Bohn, B. Reu, and A. Kleidon (2013), The Jena Diversity-Dynamic Global Vegetation Model (JeDi-DGVM): A diverse approach to representing terrestrial biogeography and biogeochemistry based on plant functional trade-offs, *Biogeosciences*, *10*(6), 4137–4177, doi:10.5194/bg-10-4137-2013.
Pfeiffer, M., A. Spessa, and J. O. Kaplan (2013), A model for global biomass burning in preindustrial time: LPJ-LMfire (v1.0), *Geosci. Model Dev.*, *6*(3), 643–685, doi:10.5194/gmd-6-643-2013.
Pinno, B. D., S. D. Wilson, D. F. Steinaker, K. C. J. Rees, and S. A. McDonald (2010), Fine root dynamics of trembling aspen in boreal forest and aspen parkland in central Canada, *Ann. For. Sci.*, *67*(7), 710–710, doi:10.1051/forest/2010035.
Prescott, C. E., L. M. Zabek, C. L. Staley, and R. Kabzems (2000), Decomposition of broadleaf and needle litter in forests of British Columbia: Influences of litter type, forest type, and litter mixtures, *Can. J. For. Res.*, *30*, 1742–1750.
Rayment, M. B., D. Loustau, and P. G. Jarvis (2002), Photosynthesis and respiration of black spruce at three organizational scales: Shoot, branch and canopy, *Tree Physiol.*, *22*, 219–229.
Reay, D. S., F. Dentener, P. Smith, J. Grace, and R. A. Feely (2008), Global nitrogen deposition and carbon sinks, *Nat. Geosci.*, *1*, 430–437.
Rich, R. L., L. E. Frelich, and P. B. Reich (2007), Wind-throw mortality in the southern boreal forest: Effects of species, diameter and stand age, *J. Ecol.*, *95*(6), 1261–1273, doi:10.1111/j.1365-2745.2007.01301.x.
Ruess, R. W., R. L. Hendrick, A. J. Burton, K. S. Pregitzer, B. Sveinbjornsson, M. E. Allen, and G. E. Maurer (2003), Coupling fine root dynamics with ecosystem carbon cycling in black spruce forests of interior Alaska, *Ecol. Monogr.*, *73*(4), 643–662, doi:10.1890/02-4032.
Ryan, M. G., M. B. Lavigne, and S. T. Gower (1997), Annual carbon cost of autotrophic respiration in boreal forest ecosystems in relation to species and climate, *J. Geophys. Res.*, *102*(D24), 28,871–28,883, doi:10.1029/97JD01236.
Sellers, P. J., et al. (1997), BOREAS in 1997: Experiment overview, scientific results, and future directions, *J. Geophys. Res.*, *102*(D24), 28,731–28,769, doi:10.1029/97JD03300.
Sheffield, J., G. Goteti, and E. F. Wood (2006), Development of a 50-year high-resolution global dataset of meteorological forcings for land surface modeling, *J. Clim.*, *19*(13), 3088–3111, doi:10.1175/jcli3790.1.
Sperry, J. S., K. L. Nichols, J. E. M. Sullivan, and S. E. Eastlack (1994), Xylem embolism in ring-porous, diffuse-porous, and coniferous trees of Northern Utah and Interior Alaska, *Ecology*, *75*(6), 1736–1752.
Steele, S. J., S. T. Gower, J. G. Vogel, and J. Norman (1997), Root mass, net primary production and turnover in aspen, jack pine and black spruce forests in Saskatchewan and Manitoba, Canada, *Tree Physiol.*, *17*, 577–587.
Strong, W. L., and G. H. la Roi (1983), Root-system morphology of common boreal forest trees in Alberta, Canada, *Can. J. For. Res.*, *13*, 1164–1173.
Ter-Mikaelian, M. T., and M. D. Korzukhin (1997), Biomass equations for sixty fice North American tree species, *For. Ecol. Manage.*, *97*, 1–24.
Terrier, A., W. J. de Groot, M. P. Girardin, and Y. Bergeron (2014), Dynamics of moisture content in spruce–feather moss and spruce–Sphagnum organic layers during an extreme fire season and implications for future depths of burn in Clay Belt black spruce forests, *Int. J. Wildland Fire*, *23*(4), A-M, doi:10.1071/wf13133.
Thornton, P. E., and N. A. Rosenbloom (2005), Ecosystem model spin-up: Estimating steady state conditions in a coupled terrestrial carbon and nitrogen cycle model, *Ecol. Modell.*, *189*(1-2), 25–48, doi:10.1016/j.ecolmodel.2005.04.008.
Trumbore, S. E., and J. W. Harden (1997), Accumulation and turnover of carbon in organic and mineral soils of the BOREAS northern study area, *J. Geophys. Res.*, *102*(D24), 28,817–28,830, doi:10.1029/97JD02231.
Vadeboncoeur, M. A. (2010), Meta-analysis of fertilization experiments indicates multiple limiting nutrients in northeastern deciduous forests, *Can. J. For. Res.*, *40*(9), 1766–1780, doi:10.1139/x10-127.
Van Bogaert, R., S. Gauthier, I. Drobyshev, K. Jayen, D. F. Greene, and Y. Bergeron (2015), Prolonged absence of disturbance associated with increased environmental stress may lead to reduced seedbank size in Picea mariana in Boreal Eastern North America, *Ecosystems*, 18(7), 1135–1150, doi:10.1007/s10021-015-9888-3.
Walko, R. L., et al. (2000), Coupled atmosphere–biophysics–hydrology models for environmental modeling, *J. Appl. Meteorol.*, *39*, 931–944.
Way, D. A., J. C. Domec, and R. B. Jackson (2013), Elevated growth temperatures alter hydraulic characteristics in trembling aspen (Populus tremuloides) seedlings: Implications for tree drought tolerance, *Plant, Cell Environ.*, *36*(1), 103–115, doi:10.1111/j.1365-3040.2012.02557.x.
Weber, M. G., and M. D. Flannigan (1997), Canadian boreal forest ecosystem structure and function in a changing climate: Impact on fire regimes, *Environ. Rev.*, *5*, 145–166.
Welp, L. R., J. T. Randerson, and H. P. Liu (2007), The sensitivity of carbon fluxes to spring warming and summer drought depends on plant functional type in boreal forest ecosystems, *Agric. For. Meteorol.*, *147*(3-4), 172–185, doi:10.1016/j.agrformet.2007.07.010.
White, M. A., P. E. Thornton, S. W. Running, and R. R. Nemani (2000), Parameterization and sensitivity analysis of the BIOME–BGC terrestrial ecosystem model: Net primary production controls, *Earth Interactions*, *4*(3), 1–84, doi:10.1175/1087-3562(2000)004 < 0003:PASAOT>2.0.CO;2.

Williams, T. G., and L. B. Flanagan (1996), Effect of changes in water content on photosynthesis, transpiration and discrimination against 13CO2 and C18O16O in Pleurozium and Sphagnum, *Oecologia*, *108*, 38–46.

Xu, X., D. Medvigy, J. S. Powers, J. Becknell, and K. Guan (2016), Hydrological niche separation explains seasonal and inter-annual variations of vegetation dynamics in seasonally dry tropical forests, *New Phytol.*, doi:10.1111/nph.14009, in press.

Yarie, J., E. Kane, and M. C. Mack (2007), Aboveground biomass equations for the trees of interior Alaska, *AFES Bull.*, *115*, 1–16.

Yi, S., A. D. McGuire, E. Kasischke, J. Harden, K. Manies, M. Mack, and M. Turetsky (2010), A dynamic organic soil biogeochemical model for simulating the effects of wildfire on soil environmental conditions and carbon dynamics of black spruce forests, *J. Geophys. Res.*, *115*, G04015, doi:10.1029/2010JG001302.

Yue, C., et al. (2013), Simulating boreal forest carbon dynamics after stand-replacing fire disturbance: Insights from a global process-based vegetation model, *Biogeosci. Discuss.*, *10*(4), 7299–7366, doi:10.5194/bgd-10-7299-2013.

Zackrisson, O., T. H. DeLuca, M.-C. Nilsson, A. Sellstedt, and L. M. Berglund (2004), Nitrogen fixation increases with successional age in boreal forests, *Ecology*, *85*(12), 3327–3334.

Zhu, Q., and Q. Zhuang (2013), Modeling the effects of organic nitrogen uptake by plants on the carbon cycling of boreal forest and tundra ecosystems, *Biogeosciences*, *10*(12), 7943–7955, doi:10.5194/bg-10-7943-2013.

Zhuang, Q., A. D. McGuire, K. P. O'Neill, J. W. Harden, V. E. Romanovsky, and J. Yarie (2002), Modeling soil thermal and carbon dynamics of a fire chronosequence in interior Alaska, *J. Geophys. Res.*, *108*(D1), 8147, doi:10.1029/2001JD001244.